

# **COMPARITIVE STUDY ON THE REMOVAL OF Cr (VI) FROM AQUEOUS SOLUTION BY BIOSYNTHESIZED AND CHEMICALLY SYNTHESIZED FERRITE NANOPARTICLES**

**Project report submitted to  
MAHATMA GANDHI UNIVERSITY, KOTTAYAM**



**for the partial fulfilment of the requirements for the award of the degree of**

**MASTER OF PHILOSOPHY**

**IN**

**PHYSICS**

**ANAKHA M**

**SMP20PHY001**



**DEPARTMENT OF PHYSICS**

**ST. TERESA'S COLLEGE (AUTONOMOUS), ERNAKULAM 682011**

**AUGUST 2022**

# **COMPARITIVE STUDY ON THE REMOVAL OF Cr (VI) FROM AQUEOUS SOLUTION BY BIOSYNTHESED AND CHEMICALLY SYNTHESED FERRITE NANOPARTICLES**

**MPhil THESIS**

**SUBMITTED BY:**

**ANAKHA M**

**Department of Physics**

**St. Teresa's College (Autonomous)**

**Ernakulam 682011**

**SUPERVISOR:**

**Dr. MARIYAM THOMAS**

**Assistant Professor**

**Department of Physics**

**St. Teresa's College (Autonomous)**

**Ernakulam 682011**

# MAHATMA GANDHI UNIVERSITY

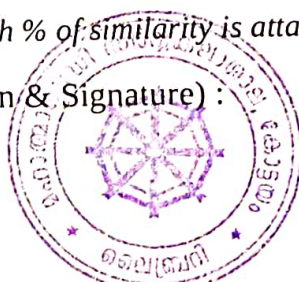
## CERTIFICATE ON PLAGIARISM CHECK


1.	Name of the Research Scholar	ANAKHA M
2.	Title of the Thesis/Dissertation	COMPARITIVE STUDY ON THE REMOVAL OF Cr (VI) FROM AQUEOUS SOLUTION BY BIOSYNTHESIZED AND CHEMICALLY SYNTHESIZED FERRITE NANOPARTICLES
3.	Name of the Supervisor(s)	Dr. Mariyam Thomas
4.	Department/Institution/ Research Centre	Department of Physics St. Teresa's College, Ernakulam
5.	Similar Content (%) identified	1% (One)
6.	Acceptable Maximum Limit	25%
7.	Software Used	Ouriginal
8.	Date of Verification	25-08-2022

\*Report on plagiarism check, items with % of similarity is attached

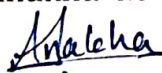
Checked by (with Name, Designation & Signature) :

V. L.  
25-8-22

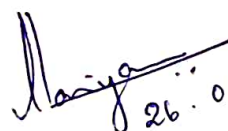


  
**LETHA ARAVIND**  
Assistant Librarian Gr.-1 in-charge  
M.G. University Library  
P.D. Hills P.O., Kottayam - 686 560

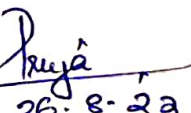
Name & Signature of the Researcher : Anakha M



Name & Signature of the Supervisor(s) : Dr. Mariyam Thomas

  
26.08.22

Name & Signature of the HoD/ HoI (Chairperson of the Doctoral Committee) :

  
26.8.22



**Dr. Priya Parvathi Ameena Jose**  
Head of the Department  
Department of Physics  
St. Teresa's College (Autonomous) Ernakulam

**Dr. Priya Parvathi Ameena Jose**  
Head of the Department  
Department of Physics  
St. Teresa's College (Autonomous) Ernakulam

### Document Information

Analyzed document ANAKHA M-COMPARITIVE STUDY ON THE REMOVAL OF Cr VI FROM AQUEOUS SOLUTION BY BIOSYNTHESIZED AND CHEMICALLY SYNTHESIZED FERRITE NANOPARTICLES.pdf (D143242456)

Submitted 8/25/2022 9:00:00 AM

Submitted by Smt. Letha Aravind

Submitter email library@mgu.ac.in

Similarity 1%

Analysis address library.mgu@analysis.arkund.com

### Sources included in the report

- W** URL: <https://pubmed.ncbi.nlm.nih.gov/26549918/>  
Fetched: 3/29/2021 6:47:31 AM 2
- W** URL: <https://www.ncbi.nlm.nih.gov/pmc/articles/PMC6480960/>  
Fetched: 10/17/2019 12:16:43 PM 2
- W** URL: <https://www.ncbi.nlm.nih.gov/pmc/articles/PMC4632970/>  
Fetched: 10/21/2019 1:30:22 PM 1

V.V.  
25-8-22

Letha Aravind  
25/8/22



**LETHA ARAVIND**  
Assistant Librarian Gr. - I in-charge  
M.G. University Library  
P.D. Hills P.O., Kottayam - 686 560

Dr. MARIYAM THOMAS  
Assistant Professor  
Department of Physics  
St. Teresa's College (Autonomous)  
Ernakulam 682011



DATE : 26/08/2022

## CERTIFICATE

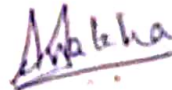
This is to certify that this dissertation entitled “**COMPARITIVE STUDY ON THE REMOVAL OF Cr (VI) FROM AQUEOUS SOLUTION BY BIOSYNTHESIZED AND CHEMICALLY SYNTHESIZED FERRITE NANOPARTICLES**” is a bonafide work carried out by ANAKHA M (Reg. No. SMP20PHY001) under my supervision and guidance in partial fulfillment of the requirements for the Degree of Master of Philosophy in Physics at St. Teresa's College (Autonomous), Ernakulam affiliated to Mahatma Gandhi University, Kottayam.

*Anneta Philip*  
20/08/2022  
Dr. ANNIETA PHILIP IC  
External Examiner

*Mariyam Thomas*  
26.08.22  
Dr. MARIYAM THOMAS  
(Supervising Guide)

# DECLARATION

I Anakha M, hereby declare that this dissertation entitled "COMPARITIVE STUDY ON THE REMOVAL OF Cr (VI) FROM AQUEOUS SOLUTION BY BIOSYNTHESED AND CHEMICALLY SYNTHESIZED FERRITE NANOPARTICLES" is based on the original work done by me at the Department of Physics, St. Teresa's College (Autonomous), Ernakulam. The work presented in this dissertation has not been submitted for the award of any other degree or diploma elsewhere.



Anakha M

Date: 26/08/2022

Place: Ernakulam

# ACKNOWLEDGEMENTS

**“I can no other answer make but thanks, and thanks, and ever thanks.”**

- *William Shakespeare*

I would like to express my deepest gratitude to my supervisor, Dr. Mariyam Thomas, Assistant Professor, Department of Physics, St Teresa's College for her expert guidance, constant support, and encouragement throughout my research work. I am sincerely indebted for her valuable suggestions and fruitful discussions in the course of this project. I could not have undertaken this journey without her advice and help. I am extremely thankful to her for giving me all the exposure I have had in this period.

I express my gratitude to Dr. Priya Parvathi Ameena Jose, Head of the Department of Physics, St Teresa's college for all the support and facilities. I express my heartfelt thanks to Dr. Sunsu Kurian for her support and advice. I express my sincere gratitude to all other teachers and non-teaching staff for their help and co-operation throughout my work.

I thank the Department of Collegiate Education (DCE), Government of Kerala for the funding provided under ASPIRE scheme.

I am extremely grateful to Dr. Derry Holaday, Assistant Professor, Department of Chemistry, Department of Chemistry for providing me with all the facilities, support, and guidance in the course of work as a part of ASPIRE scheme. I express my deep sense of gratitude to Ms. Akshaya Pavithran, MPhil Scholar, Department of Chemistry, University of Calicut for being there with me the whole time and helping me in all means during the course of work. I would like to thank all other research scholars and faculty members in the department for the love and care they have shown to me.

I thank Sophisticated Test and Instrumentation Centre (STIC), Cochin University of Science and Technology for getting the first set of XRD characterization done. I sincerely thank Central Sophisticated Instrumentation Facility, University of Calicut for their help in XRD and SEM characterizations and ICP MS studies. I thank the Department of Chemistry, University of Calicut for getting FT-IR characterization done.

I am very much grateful to Mrs. Thanooja Nizam, Research Scholar, Department of Physics, Mar Ivanios College, Kerala University, my senior for her suggestions and every possible

help at every stage of this work. I thank my batchmates Mrs. Merly Ann Peter, Mrs. Rajani Nair, Ms. Anjaly Ravi, Sr Achal Grace, and Ms. Farzana for their support and help. I would like to thank Ms. Pauline Jesna Joseph and Ms Ann Sivna Rose, MSc students for their timely help. I thank everyone for all the joyful moments.

Words fail to express my love and gratitude towards Mr. Manu Varghese who has been there with me in all ups and downs with his support and encouragement in the course of work. I would like to thank Mr. Pradeep P for his encouragement and timely pieces of advice. I sincerely thank my hostel mates especially Ms. Anju Johny for staying with me all night just to make sure that I don't feel lonely. I express my love and gratitude to Ms. Gowri, Ms. Nandana, and Ms. Afsana for their help and support. I extend my gratitude to my friends Mr. Yegnesh N Iyer and Mrs. Sajana Venkideshwaran for their timely support.

Family is not an important thing, it's everything. My family is the major support system and is the reason for all the achievements in my life. I take this opportunity to thank my parents, sister, and all other family members for their love and blessings showered upon me. I thank them for their unconditional love, support, and trust in me.

I thank God almighty for choosing me to be in this place.



## **POSTER PRESENTATION**

- Presented a poster entitled **“EXPLORING GREEN ROUTE TO SYNTHESIZE METAL FERRITE NANOPARTICLE USING POTENTIAL NATURAL EXTRACTS”** in the International Conference on Frontiers in Chemical Sciences-2022 (FCS-2022) held at the Department of Chemistry, University of Calicut during 03-05 March 2022.
  
- Presented a poster entitled **“A STUDY ON THE EFFECT OF SYNTHESIS METHOD ON ADSORPTION PROPERTIES OF NANOMETAL FERRITES”** in the Annual Physics Symposium, APS 2022 organized by the Department of Physics, St. Teresa’s College, Ernakulam on 18<sup>th</sup> March 2022.

## ABSTRACT

The present work is an attempt on the synthesis of  $\text{ZnFe}_2\text{O}_4$  nanoparticles using the aqueous plant extract by employing the co-precipitation method and its feasibility towards its adsorptive removal of  $\text{Cr(VI)}$  ions from synthetic water prepared were examined. The aqueous extract of *Zingiber officinale* was used as the stabilizing agent. The as-synthesized  $\text{ZnFe}_2\text{O}_4$  nanoparticles were characterized using various characterization techniques. Structural and phase identification was studied from the X-ray diffraction pattern revealed the spinel structure of the sample. The functional groups attached with the synthesized  $\text{ZnFe}_2\text{O}_4$  nanoparticles were identified from the Fourier Transform Infrared spectrum. The morphology of synthesized magnetic nanoparticles was analyzed using Scanning Electron Microscope which confirms the less agglomeration of  $\text{ZnFe}_2\text{O}_4$  nanoparticles with spherical morphology.

The adsorptive properties of  $\text{ZnFe}_2\text{O}_4$  samples on  $\text{Cr(VI)}$  were studied by performing batch adsorption studies with optimum values of the factors affecting the heavy metal adsorption viz contact time, temperature, adsorbent dosage, and initial ion concentration. The concentration of  $\text{Cr(VI)}$  after the interaction of  $\text{ZnFe}_2\text{O}_4$  with the prepared  $\text{Cr(VI)}$  solution was estimated by Inductively Coupled Plasma Mass Spectrometer. The adsorption efficiency is calculated and compared with that of chemically synthesized  $\text{ZnFe}_2\text{O}_4$ . The bio  $\text{ZnFe}_2\text{O}_4$  sample showed improved adsorptive properties for the removal of  $\text{Cr(VI)}$  from its aqueous solution when compared with the chemically prepared  $\text{ZnFe}_2\text{O}_4$  sample.

# CONTENT

## Chapter 1

### INTRODUCTION

1.1 Heavy metals	2
1.1.1 Pollution and effects	2
1.1.2 Sources	2
1.1.3 Effect of Heavy Metal consumption on human health	3
1.2 Why Chromium?	5
1.2.1 Environment health and human exposure	6
1.2.2 Guideline values	6
1.3 Removal of heavy metal from water	6
1.4 Ferrites	13
1.4.1 Classification of ferrites	14
1.4.2 Spinel ferrites as adsorbents	21
1.5 Nano metals in wastewater treatment	24
1.6 Project outline	24
1.7 Literature Review	25
<b>References</b>	<b>27</b>

## Chapter 2

### EXPERIMENTAL TECHNIQUES

2.1 Synthesis method: Co-precipitation method	32
2.1.1 Synthesis procedure	33
2.2 Preparation of synthetic wastewater	34
2.3 Adsorption studies	35
2.4 Characterization techniques	36
2.4.1 X-Ray Diffraction	37
2.4.2 Fourier Transform Infrared Spectroscopy	41

2.4.3	Scanning Electron Microscopy	44
2.4.4	Inductively coupled Plasma Mass Spectroscopy	51

## References

56

## Chapter 3

### RESULTS AND DISCUSSION

3.1	Phase identification: X-Ray Diffraction	58
3.1.1	Estimation of average crystallite size	60
3.1.2	Determination of lattice parameters	62
3.2	Identification of functional groups: Fourier Transform - Infrared Spectroscopy	64
3.3	Morphological Studies: Scanning Electron Microscopy	65
3.4	Adsorption Studies: ICP MS	66
	References	70

## Conclusion

71

## Future Scope

72

## FIGURES

Fig 1.1:	Contamination of water bodies by industrial effluents	2
Fig 1.2:	Contamination sources, Guideline values and effect on Health	4
Fig 1.3 (a):	Spinel Ferrites	17
Fig 1.3 (b):	Normal spinel ferrite	17
Fig 1.3 (c):	Inverse spinel ferrite	18
Fig 1.3 (d):	Intermediate spinel ferrite	19
Fig 1.4	Garnet ferrite	19
Fig 1.5:	Hexagonal ferrite	20
Fig 1.6:	Ortho ferrite	21
Fig 2.1(a):	Reflection of X-Rays from parallel crystal planes	38
Fig 2.1(b):	Basic components of X-Ray Diffractometer	41
Fig 2.2 (a):	Michaelson's Interferometer	43
Fig 2.2 (b):	Schematic diagram of FTIR.	44
Fig 2.3 (a):	Signals generated by the interaction of specimen electron beam in the scanning electron microscope	46
Fig 2.3 (b):	Schematic of SEM	49
Fig 2.4 (a):	Ion source and interface in ICP MS	53
Fig 2.4 (b):	Schematic diagram of ICP MS	54
Fig 2.4 (c):	ICP MS instrument	55
Fig 3.1 (a):	X-Ray diffraction pattern of $ZnFe_2O_4$ nanoparticles calcined at different temperatures	59
Fig 3.1 (b):	X-Ray diffraction pattern of $ZnFe_2O_4$ nanoparticles calcined at $400^{\circ}C$	60
Fig 3.2 :	Fourier Transform Infrared pattern of $ZnFe_2O_4$ Nanoparticles	64

Fig 3.3 (a):	SEM image of Bio ZnFe <sub>2</sub> O <sub>4</sub> nanoparticles	65
Fig 3.3 (b):	SEM image of Sol-gel synthesized ZnFe <sub>2</sub> O <sub>4</sub> nanoparticles	66
Fig 3.4:	Equilibrium concentration of Cr <sup>6+</sup> for contact time, temperature, adsorbent dosage, and initial ion concentration respectively	68

# TABLES

Table 1:	Detection limit of various elements	52
Table 2:	Comparison of adsorption efficiency	69

# PREFACE

Chapter 1 narrates with the issue of water pollution and the importance of wastewater management in the current scenario. The role of heavy metals in polluting the water, their sources, and their effects on human health are well explained. The effect of Chromium content in water, its health hazards, and its provisional guideline value are discussed. This chapter also discusses various methods of heavy metal removal and also explains why adsorption has been chosen. Ferrites have been a matter of study in wastewater treatment because of their properties. This is also dealt with in this chapter.

Chapter 2 describes the experimental procedure in detail. The co-precipitation technique was employed for the synthesis of  $\text{ZnFe}_2\text{O}_4$  nanoparticles. The new approach in the synthesis by employing bio extract is been discussed here. The calcination temperature was optimized to  $400^\circ\text{C}$ . The synthesized metal ferrite nanoparticles were characterized using XRD, FT-IR, and SEM. The adsorptive properties of the ferrites were evaluated from ICP MS. The theory and instrumentation of the characterization techniques are well explained.

Chapter 3 includes results and discussions. The results from the XRD, FTIR, and SEM are discussed and analyzed. The optimized values of the factors affecting the adsorption mechanism which are previously reported were used to compare the adsorption efficiency with that of the chemically synthesized  $\text{ZnFe}_2\text{O}_4$  sample.



# CHAPTER 1

## INTRODUCTION

Water is the foundation of human civilization. The absence of water will wipe out the whole life on earth. The existence and survival of all living things require water as life is dependent on water, hence for the smooth functioning of the ecosystem, water is inevitable<sup>[1]</sup>.

The building material for cells, tissues, and organs which is 70% of the human body's weight, also the most important constituent of blood and body fluid makes water an integral part of our existence. The balance of body fluids and body temperature is maintained by water and it also aids many biological processes and also has a major role in the production of lubricating fluids<sup>[1]</sup>.

Freshwater which is fit for consumption is only 0.014 % of all water present on earth, of which 36 % of freshwater of 14,000 km<sup>3</sup> is used by humans. In such a scenario, water fit for consumption is to be made available, to meet the needs of the whole world's population. Uneven geographic distribution and unequal condition results in scarcity of fresh water in some parts of the world. The exponential increase in human population and quick urbanization along with followed industrialization had escalated the water scarcity issue<sup>[1]</sup>.

Human-induced water scarcity along with the prevailing scarcity has become a major concern<sup>[1]</sup>. The pollution that is caused by water has not only affected the humans but also all living beings too. Water runoff, untreated after agricultural and domestic activities and industrial disposal result in the contamination of water bodies and that which are connected to<sup>[1]</sup>.

There are several type of pollutants viz. heavy metals, pathogens, dyers and surfactants, and radioactive substances that contribute to water pollution and makes it unfit for consumption. Consumption of this water is hazardous to living organisms<sup>[1]</sup>.



Fig 1.1: Contamination of water bodies by industrial effluents<sup>[2]</sup>

## **1.1 HEAVY METALS**

### **1.1.1 Pollution and Effects**

A metal or a metalloid that has an atomic density higher than  $4000 \text{ Kg/m}^3$ , is a heavy metal <sup>[1]</sup>. They have relatively high density and have toxic nature even at lower concentrations Their atomic density can vary from  $4\text{g/cm}^3$  and it's five times or more or even greater than water <sup>[3]</sup> within the permissible limits, heavy metals such as Fe, Zn, Ni, and Mo has growth enhancing ability in plants. Heavy metals viz. As, Hg, Pb, and Cd are not required for plant/ animal health, moreover its consumption beyond a safe limit has hazardous consequences on health <sup>[1]</sup>. Chromium is a carcinogen and is harmful even when it's of lower concentration and is a threat to living beings <sup>[4]</sup>. Heavy metals are non-biodegradable in nature and hence elimination is difficult <sup>[1]</sup>. Hence, they reach every living organism through the food chain and bioaccumulate over a period of time <sup>[3]</sup>.

### **1.1.2 Sources**

Heavy metal concentration increases in the environment through both natural and anthropogenic activities <sup>[3]</sup>.

The natural occurrence of heavy metals in water depends on the plant's geology, geochemical characteristics, and hydrology. Weathering and sedimentary rocks viz dolomite, sandstone, and limestone pollute the water by the release of heavy metals. Igneous rock interaction with water also contributes to heavy metals resulting in water pollution. The

dissolutions of minerals/ore of heavy metals also result in water pollution. Other factors that contribute to pollution are volcanic eruptions, vegetation, and forest fires <sup>[5]</sup>.

Chemicals based on pharmaceuticals, fertilizers, paints, and pesticides produce wastewater rich in heavy metals. The manufacturing process includes electroplating, battery recycling, metal smelting, and other industrial causes that results in the release of heavy metals into the environment. Automobiles and other industries release combustion exhaust that contains lead (Pb), arsenic (As), chromium (Cr), and Mercury (Hg) in the soil. This reaches the water bodies and the surface runoff water contaminates the groundwater too <sup>[1]</sup>. In such a scenario, an increase in such activities will enhance the pollution to a great extent. Moreover, the concentration of the water distribution system also contributes to heavy metals in the water bodies <sup>[1]</sup>.

### **1.1.3 Effect of Heavy Metal consumption on human health**

Inhalation, oral intake, and chemical exposure are the three main ways by which heavy metals reach the human body. Through oral consumption of heavy metal contaminated water, they find their way to get inside the human body. Consumption of heavy metals within a permissible limit causes no harm but results in various health issues if otherwise. It doesn't mean that any one or few heavy metals beyond the limit value cause no harm, one or more heavy metals beyond the permissible limit is a threat to health. Chronic intake of heavy metals results in high risks of getting cancer, liver and kidney problems, heart disease, lung problems, bladder and gastrointestinal problems, etc. It even changes the blood composition and results in damage to internal organs. Heavy metal consumption also causes harm to cognitive development and the growth of the central nervous system, along with abnormal bone and brain development. Heavy metals have the capability of accumulating in lipids and result in fatal problems. An increase in the risk of stillbirth and congenital disabilities is seen in pregnant women due to the intake of heavy metals <sup>[1]</sup> The following fig shows some heavy metals, their source, their permissible value, and their impacts on human health is shown.

S. no.	Heavy metal	Heavy metal ion	Guideline value	Impacts on human health	Contamination sources
1	Aluminium	Al(III)	0.9 mg/l	<ul style="list-style-type: none"> <li>Anaemia</li> <li>Cardiac arrest</li> <li>Nervous system disorders</li> <li>Osteomalacia</li> <li>Glucose intolerance</li> </ul>	<ul style="list-style-type: none"> <li>Water treatment processes</li> <li>Water purification chemicals</li> </ul>
2	Antimony	Sb(III)	0.02 mg/l	<ul style="list-style-type: none"> <li>High cholesterol</li> <li>High glucose in the blood</li> </ul>	<ul style="list-style-type: none"> <li>Occurs naturally in ground</li> <li>Manufacturing of Flame retardants</li> <li>Manufacturing processes</li> <li>Natural weathering of rocks</li> <li>Industrial and municipal waste</li> <li>Natural deposits</li> <li>Agricultural activities</li> <li>Industrial practices</li> <li>Volcanic emissions</li> </ul>
3	Arsenic	As(III) and As(V)	0.01 mg/l	<ul style="list-style-type: none"> <li>Arsenicosis</li> <li>Thickening of the skin</li> <li>Stomachache</li> <li>Numbness of hands and feet, partial paralysis</li> <li>Nausea, vomiting and diarrhoea</li> <li>Blindness</li> <li>Skin, lungs, kidney, bladder, liver, nasal passages, or prostate cancer</li> </ul>	<ul style="list-style-type: none"> <li>Natural sources</li> <li>Industrial emissions</li> <li>Anthropogenic activities</li> </ul>
4	Barium	Ba(II)	1.3 mg/l	<ul style="list-style-type: none"> <li>Vasoconstriction</li> <li>Peristalsis</li> <li>Convulsions</li> <li>Paralysis</li> <li>Atherosclerotic heart disease</li> <li>Total cardiovascular disease</li> </ul>	<ul style="list-style-type: none"> <li>Natural sources</li> <li>Industrial emissions</li> <li>Anthropogenic activities</li> </ul>
5	Cadmium	Cd(II)	0.003 mg/l	<ul style="list-style-type: none"> <li>Chronic renal failure</li> <li>Kidney failure</li> <li>Anaemia</li> <li>Anosmia</li> <li>Cardiovascular diseases</li> <li>Osteoporosis</li> <li>Hypertension</li> <li>Acute and chronic intoxications</li> </ul>	<ul style="list-style-type: none"> <li>Naturally present in the soil</li> <li>Atmospheric deposition</li> <li>Industrial or agricultural activities</li> <li>From leaching, erosion and harvested crops</li> </ul>
6	Chromium	Cr(VI)	0.05 mg/l	<ul style="list-style-type: none"> <li>Liver and kidney disorders</li> <li>Dermatitis</li> <li>Respiratory issues</li> </ul>	<ul style="list-style-type: none"> <li>Occurs naturally in ground</li> <li>Old mining operations</li> <li>Industrial waste disposal</li> <li>Natural occurrences</li> <li>Anthropogenic activities</li> </ul>
7	Cobalt	Co(II)	0.05 mg/l	<ul style="list-style-type: none"> <li>Trouble in breathing</li> <li>Asthma</li> <li>Respiratory issues</li> <li>Pneumonia</li> <li>Wheezing</li> </ul>	<ul style="list-style-type: none"> <li>Natural deposits in rock and soil</li> <li>Corrosion in household plumbing</li> <li>Iron coagulants</li> <li>Corrosion of steel and cast iron pipes</li> </ul>
8	Copper	Cu(II)	2.0 mg/l	<ul style="list-style-type: none"> <li>Mild gastrointestinal distress</li> <li>Permanent liver or kidney damage</li> </ul>	
9	Iron	Fe(III)	0.2 mg/l	<ul style="list-style-type: none"> <li>Dizziness</li> <li>Low blood pressure</li> <li>Headache and fever</li> <li>Shortness of breath</li> <li>Fluid in the lungs</li> <li>Jaundice</li> <li>Seizures</li> </ul>	
10	Lead	Pb(II)	0.01 mg/l	<ul style="list-style-type: none"> <li>Neurodevelopmental effects</li> <li>Renal disorders</li> <li>Cardiovascular diseases</li> <li>Hypertension</li> <li>Adverse pregnancy outcomes and infertility</li> </ul>	<ul style="list-style-type: none"> <li>Corrosion of household plumbing and water distribution systems</li> </ul>
11	Manganese	Mn(II)	0.1 mg/l	<ul style="list-style-type: none"> <li>Neurological, cognitive and neuropsychological effects</li> </ul>	<ul style="list-style-type: none"> <li>Occurs naturally</li> <li>Under low oxygen conditions in the depth of water bodies</li> <li>Agricultural runoff</li> <li>From seepage from landfills</li> </ul>
12	Mercury	Hg(II)	0.006 mg/l	<ul style="list-style-type: none"> <li>Impaired brain functions and neurological disorders</li> </ul>	<ul style="list-style-type: none"> <li>Industrial activities</li> </ul>
13	Nickel	Ni(II)	0.07 mg/l	<ul style="list-style-type: none"> <li>Growth retardation in infants</li> <li>Complications in pregnancy</li> <li>Endocrine system disruption</li> <li>Nausea, vomiting and diarrhoea</li> <li>Giddiness and physical tiredness</li> <li>Headache and exhaustion</li> <li>Improper breathing</li> </ul>	<ul style="list-style-type: none"> <li>From fittings such as chromium-plated taps</li> <li>From stainless steel well materials</li> </ul>
14	Silver	Ag(I)	0.05 mg/l	<ul style="list-style-type: none"> <li>Potential to damage DNA</li> <li>Lowered blood pressure</li> <li>Vomiting and diarrhoea</li> <li>Stomach problems</li> <li>Respiration issues</li> <li>Stomach cramps</li> <li>Nausea and vomiting</li> </ul>	<ul style="list-style-type: none"> <li>Through natural processes</li> <li>Weathering of rocks</li> <li>Erosion of soils</li> </ul>
15	Zinc	Zn(II)	5.00 mg/l		<ul style="list-style-type: none"> <li>Corrosion of piping and fittings</li> </ul>

Fig 1.2: Contamination sources, guideline value,<sup>[1]</sup> and effects on health of heavy metals<sup>[1]</sup>

The International Agency of Research on cancer declares chromium as the most powerful carcinogenic agent that can even modify the DNA transcription process which results in major chromosomal aberrations, chromium in water also causes serious environmental problems <sup>[6]</sup>.

## 1.2 WHY CHROMIUM?

Environmental pollution caused by chromium is a major issue in recent years <sup>[7]</sup>. Among all regulated toxic elements present in the environment, chromium stands out as they exist in two different oxidation states, <sup>[8]</sup> i.e., as a trivalent cation Cr (III) and as an anion in the hexavalent state Cr(VI) <sup>[7]</sup>. Also, they are regulated in different ways based on their toxicities. Other heavy metals viz Pd, Cd, and As are regulated based on their concentration not as per the oxidation state <sup>[8]</sup>.

Cr (III) has a positive role in the functioning of living beings. They ensure the correct glucose metabolism in animals and undergo complexation with several substances present in the environment very easily. In contrast to this, Cr (VI) compounds are highly toxic and their intake caused many health issues. Pneumonia and asthma are caused as a result of inhalation. Skin contact with Cr (VI) causes allergies and dermatoses. The International Agency for Research on Cancer (IARC) has classified Cr (VI) compounds in the Bz group which implies that they are carcinogenic and mutagenic in humans. Cr (VI) is 1000 times more toxic than Cr (III) <sup>[9]</sup> and the United States Environmental Protection Agency (USEPA) classifies hazardous waste as of it consist of chromium ( 40 CFR 261.4) but excludes those from this if the leachable chromium is not chromium (40 CFR 261.94) <sup>[8]</sup>.

The reduction of Cr (VI) to Cr (III) results in the formation of free radicals. This property along with its strong oxidizing properties roots for the toxic nature of Cr (VI). As Cr (VI) compound shows high mobility, and solubility along with its bioavailability, their toxicity is to be considered a major issue, hence it has to be amplified. Cr (VI) can easily penetrate into the cell membrane. Once they are inside the cells, they react with the enzymes that are responsible for phosphate and sulfate metabolism. The normal functioning of nucleic acid viz DNA and RNA are also disturbed by chromium. This results in cell anomalies <sup>[9]</sup>.

### **1.2.1 Environment levels and Human Exposure**

#### **i) Water**

The average Cr(VI) concentration in drinking water samples in the USA was 0.2-2µg/L and that of the rainwater was in the range of 0.2-1µg/L. The seawater has an average concentration of 0.04-0.5µg/L. The total chromium concentration in groundwater is less than 1µg/L. But, the concentration of chromium in surface water was found to be 8µg/L which indicates the influence of industrial activity on water pollution <sup>[10]</sup>.

#### **ii) Air**

Chromium concentration of air in remote areas is 0.005-2.6ng/m<sup>3</sup> while ambient air showed very little concentration of chromium which is less than 300 ng/m<sup>3</sup>. Chromium concentration in urban areas was above 10 ng/m<sup>3</sup>. Tobacco smoke also contributes to a concentration of chromium in indoor air <sup>[10]</sup>.

#### **iii) Food**

Food is the main source of chromium exposure. It is found to contain a total chromium concentration of less than 0.0005-1.3µg/g. Meat, seafood, cereal products, tea, cheese, and some fruits and vegetables show a high concentration of chromium i.e., greater than 0.1µg/g. Drinks with beverage content viz beer, wine, and spirits have a much higher concentration of chromium viz 450, 300, and 135µg/L respectively <sup>[10]</sup>.

### **1.2.2 Guideline Values**

Guideline value is a proposal based on current analytical methods. It is based on current treatment technologies, measures done by various analytical methods, and toxicological values. The main intention of guideline value is to protect from both carcinogenic Cr (VI) and non-carcinogenic Cr (III) <sup>[10]</sup>.

The guideline value for total chromium in drinking water is 50µg/L. This level is assumed to be a safer level from health risks <sup>[10]</sup>.

## **1.3 REMOVAL OF HEAVY METAL FROM WATER**

Several methods of wastewater management techniques that include physical, chemical, and biological procedures are employed to make contaminated water into water that is fit for consumption. This includes adsorption, electrochemical treatments, ion-exchange mechanism flotation, reverse osmosis, membrane filtration, evaporation, oxidation

precipitation, and biosorption. Out of these some may be efficient enough to remove pathogens but may fail to remove heavy metals and vice versa <sup>[1]</sup>.

### **1. Ion exchange mechanism**

In the Ion exchange mechanism, the exchange of ions between the substrate and the surrounding medium takes place. As this method is reversible, it is possible to reverse the exchanging material several times. Ion exchange resins are polymer matrices that are non-magnetic and insoluble in most of the aqueous and organic solvents, that are used for this process. These are manufactured in spherical, stress and strain-free conditions such that they are resistant to physical degradation. The ion exchange resins have a cross-linked polymer matrix and the functional group gets attached to them through covalent bonding. There are two types of resins mainly cation exchange resins and anion exchange resins, that have cations and anions as counter ions <sup>[11]</sup>. So, the negative ion from the polymer is replaced by the positive charged heavy metal ions. The ion exchange resins are classified according to the type of functional group and exchange ions. They are:

- 1) Strong acidic resins containing sulphonic acid groups and
- 2) Weak acidic resins that contain carboxylic acid groups<sup>[11]</sup>.

Strong acidic resins dissociate over a vast pH and attain maximum sorption, whereas weak acidic resins attain a maximum sorption capacity at a pH greater than 7. Another class of resins is amphoteric resins which can exchange either cations or anions as per the pH of the surrounding medium. The separation of ions is dependent on the minute differences in affinity of the ions and the result of this process is the separation of metal ions from solution. The efficiency of this process depends on the nature and characteristics of the resins <sup>[11]</sup>.

### **2. Flootation**

In the process of Ion floatation, surface active agents are used to turn the metallic ions present in the wastewater hydrophobic, and these hydrophobic species are removed by introducing air bubbles onto the medium. A typical surfactant molecule will have a polar ionic head that attaches to a metal ion and the nonpolar hydrocarbon chain which is hydrophobic gets exposed to the solution. The metal ion surfactant assembly float to the surface on the introduction of air bubbles onto the floatation cell. This occurs due to the interaction between the hydrocarbon chain and air bubbles. The complex that floats on the surface is removed as a froth, and thus the heavy metal removal is achieved. Therefore, the surfactant molecules are called collectors. For the floatation process to be effective, the size of the air bubble that is to

be introduced in the floatation cell should be in the range of a few 100  $\mu\text{m}$  to provide the required surface area for collection. The size of the bubbles is controlled by the source detergents called frothers, that in turn reduce the air to water interfacial tension<sup>[12]</sup>.

A large metal ion to water ratio in the froth phase implies a successful heavy metal removal, which means that the floatation process is evaluated not by just considering the metal content in the froth, but by considering the relative recoveries of metal ions and water from the floatation cell <sup>[12]</sup>.

### **3. Reverse osmosis**

The process of reverse osmosis forces a solution using pressure to push the solvent through a membrane and the solute remains on one side of the membrane. By applying a pressure in excess of osmotic pressure, the solvent is forced to move from a region of lower concentration to a higher concentration through a membrane. This process is the exact opposite of the normal osmosis process, where the solvent moves to a higher concentration region from a lower concentration region in the absence of external pressure. This process makes use of a semi-permeable membrane that only allows solvents, not the solutes to pass through it <sup>[13]</sup>.

### **4. Bio sorption**

This process involves a biological technique for the removal of pollutants present in the wastewater. There, microorganisms are used, that settle down the solids in the solution. Activated sludge is the most common technique that uses microorganisms for the treatment process. They break down the organic material and this is followed by agitation. Then it is allowed to settle down<sup>[14]</sup>.

As the name implies, biosorption includes adsorption and precipitation reactants. The ions from the solution phase are converted into a solid phase by a group of processes and are called sorption<sup>[14]</sup>.

Biological treatments are economical, environment friendly, and efficient for wastewater treatment <sup>[14]</sup>.

### **5. Electrochemical treatments**

The different electrochemical method includes:

1. Electrochemical reduction
2. Electrofloatation



### 3. Electrooxidation

### 4. Electrocoagulation<sup>[15]</sup>.

Oxidation occurs at the anode and reduction occurs at the cathode in an electrochemical system. The electrons travel from anode to cathode. Simultaneous oxidation and reduction take place and this is meant by redox reaction, whose result is the purification of water and by the elimination of heavy metal ions<sup>[15]</sup>.

The removal efficiency of specific metal ions depends on the type of method and the anode and cathode materials chosen<sup>[15]</sup>.

#### **1. Electrodeposition**

The surface of the cathode is the site for the deposition of targeted atoms or molecules. Carbon-based or sulfur mixtures under acidic conditions of various ratios are best for heavy metal removal from wastewater. Reactor design and operating conditions are the other factors that improve the efficiency of wastewater treatments. One of the major drawbacks of this method is the energy consumption required for this process<sup>[15]</sup>.

#### **2. Electro floatation**

In this technique, insoluble electrodes are used for the electrolysis of water, followed by the floatation method to aid the treatment process. The electrodes are insoluble, non-corrosive, and highly catalytic with the anions in the electrolyte. The oxygen evolution is a barrier to heavy metal removal<sup>[15]</sup>.

#### **3. Electrooxidation**

This technique has two approaches, direct and indirect. The direct method is simple whereas indirect oxidation depends upon the ion concentration but does not depend on current intensity. A polymeric layer is formed on the anode surface when electron exchange takes place between the anode and pollutants. As a result, the oxides of constraints will be there in the solution<sup>[15]</sup>.

#### **4. Electrocoagulation**

In this method, usually steel or Al electrodes are used due to their non-toxic nature. The cations of the anodic metal are dissolved and this is followed by hydroxo complex formation. The phase separation of the aggregate is then carried out<sup>[15]</sup>.

The drawback of this method is the largescale application using low, energy consumption<sup>[15]</sup>.

## 6. Adsorption

Recent studies in the field of heavy metal removal focus on a technique that make use of naturally occurring and synthetic adsorbents. The advantages and disadvantages of each technique to remove metal ions can be understood through this<sup>[16]</sup>.

Removal of the adsorbents has been a major concern over time. Adsorption is considered the most suitable technique for water management because of its effectiveness and economical nature<sup>[16]</sup>. Adsorption ensures less expensive, efficient removal of heavy metals and simple treatment procedures. Another feature of the adsorption method is the regulation of the adsorbed metal ions<sup>[15]</sup> just by adjusting pH, which aids to obtain the adsorbents back after adsorption, and hence it can be recycled several times<sup>[16]</sup>.

### 6.1 Mechanism

Adsorption by definition is a process of mass transfer that involves the accumulation of substances at the interface of two phases and this can be liquid-liquid, gas-liquid, gas-solid, or liquid-solid<sup>[17]</sup>. The substance that gets adsorbed to the adsorbent is termed an adsorbate<sup>[18]</sup> and the material that adsorbs that substance is adsorbent<sup>[17]</sup>. Depending on these constituents in both adsorbents and adsorbates, their properties vary. The removal of any kind of pollutants from wastewater is based on the type of constituents of the adsorbent<sup>[17]</sup>.

There are two ways by which the adsorption of molecules takes place on the surface of the adsorbent. They are physisorption and chemisorption<sup>[18]</sup>. If a physical nature is seen in the interaction between the solid surface of the adsorbent and adsorbed molecule, then this process is termed physisorption. In such a case Van der Waals's forces are responsible for the interaction, which means they are reversible. A temperature close to the critical temperature of the adsorbate is required. For chemisorption, the interaction between the adsorbent and the adsorbate is due to chemical bonding clearly, the attractive forces will be high and hence it can be hardly removed. Physisorption and chemisorption can occur simultaneously under suitable conditions<sup>[17]</sup>.

The adsorption process is affected by the following factors:

1. Surface area
2. Nature and initial concentration of adsorbate
3. Solution pH

4. Temperature
5. Interfacing substances
6. Nature and dose of adsorbent<sup>[17]</sup>.

Adsorption is a surface phenomenon. So, the area available for adsorption out of the total surface area has a huge influence on how much adsorption will occur. Moreover, the more porous the adsorbents are, the greater will be the adsorption process attained per unit weight of the solid adsorbent. The pores of the adsorbent molecular surface will be of molecular dimensions and hence so will the surface area <sup>[17]</sup>. There will be more sites for the adsorption to occur. Another major factor that influenced the extent of adsorption is pH. This is because the surface charge distribution can be altered by bringing a change in pH <sup>[17]</sup>.

Adsorption processes are exothermic hence a great extent of the adsorption process is seen at lower temperatures <sup>[17]</sup>.

## **6.2 Adsorbents: Various Types**

### **i. Carbon-based adsorbents**

Activated carbons, carbon nanotubes of graphene which are carbon-based nanoporous adsorbents, are used extensively in heavy metal removal techniques due to their large surface area. The heavy metal uptake by the surface functional groups is enhanced by the carbon surface charges. There are several modification methods to enhance the specific surface area, pore structure, and adsorption capacity, but somehow these properties are related to the nature of adsorbent materials. Surface modification techniques that are employed these days demand high temperature, pressure, strong acid-base conditions, and intensive oxidation-reduction reactions. These conditions result in the cost of carbon base adsorbents as the preparation technique is complex. So, a more cost-effective, environment-friendly technique is much awaited <sup>[15]</sup>.

### **ii. Chitosan based adsorbents**

Chitosan is a natural adsorptive polymer that has amino (-NH<sub>2</sub>) and hydroxyl (-OH) groups and shows a greater affinity towards pollutants. But the regeneration is not sufficient because of its low mechanical strength and poor stability. Moreover, they are less porous which implies less surface area highly crystalline, and show resistance to mass transfer.

Therefore, they require structural and chemical modifications. A remarkable increase in the adsorption capacity by grafting, a method that involves covalent bonding of functional groups [15].

### **iii. Mineral Adsorbents**

Zeolites, silica, and clay are considered better adsorbents for water purification in an economical way. Clay shows extraordinary cation exchange selectively. Moreover, washing and thermal treatment enlarge the pore size, pore volume, and specific surface area thereby enhancing the adsorption efficiency. Though natural mineral adsorbents are less expensive after a few cycles, a decrease in their removal efficiency is observed. Difficult modification methods will enhance the cost, in addition to that few chemicals are also released as byproducts [15].

### **iv. Biosorbents**

The presence of various functional groups like carboxyl, amino, hydroxyl, etc. on the surface of adsorbents enhances the process of biosorption. Unlike others, the surface of biosorbents and pollutant interactions can be aggregation, ion exchange, electrostatic interaction, and reduction /oxidation. The surface charge density of the biosorbent and the ionization of functional groups at the surface is affected by pH. Cations show more stability at lower pH levels and are prone to bonding at biosorbent surfaces, but on higher pH levels, there are higher pH levels, and there are higher chances for precipitation<sup>[15]</sup>.

Biosorbent materials offer more vacant sites which enhance the adsorption. But at higher temperatures, the removal efficiency reduces [15].

### **v. Magnetic Adsorbents**

Magnetic adsorbents are a class of adsorbent materials with  $\text{Fe}_3\text{O}_4$  as its chief content. The adsorption process involving magnetic adsorbents can be influenced or controlled by an external magnetic field, thus by ensuring retrieval of the adsorbents and their reusability. Low cost, simple synthesis procedure, and abundant surface charge makes magnetic adsorbent an attractive class to be chosen as effective adsorbents [15].

Spinel ferrite nanoparticles have been a major attraction because of their cost-effective and efficient nature [19]. Separation of the adsorbents after the waste treatment process is a major concern. But here in the case of spinel ferrite nanoparticles application of an external

magnetic field will retrieve the spent adsorbents because of the magnetic nature of spinel ferrites. Magnetic separation is far superior to conventional filtration and centrifugation processes. The spinel ferrite nanoparticle adsorbents mediated adsorption process can be considered as an improvised version of the adsorption mechanism <sup>[19]</sup>.

Moreover, the adsorption process can be done by tuning the pH of the environment which enabled the recyclability property of ferrites. Properties of spinel ferrites depend on the synthesis technique, which can be done by several methods <sup>[20]</sup>. The co-precipitation technique ensures spinel ferrites nanoparticles of high purity with no aggregation and the magnetic property is assured <sup>[21]</sup>.

Out of the investigated spinel metal ferrites, done by Nizam, Thanooja, et al. "Adsorption efficiency of sol-gel derived nano metal ferrites,  $MFe_2O_4$  ( $M= Ni, Zn, Cu$ ) on the removal of Cr (VI) ions from aqueous solution." *Journal of Sol-Gel Science and Technology* 101.3 (2022): 618-629. Zinc ferrites showed better performance in the adsorption of Cr (VI) ions <sup>[16]</sup>.

#### 1.4 FERRITES

Ferrites are a class of magnetic oxides that contain iron oxides as their main constituent <sup>[22]</sup>. They are ceramic materials and exhibit ferrimagnetic behavior <sup>[23]</sup>. Magnetite ( $Fe_3O_4$ ) was the first ever ferrimagnetic material known to man<sup>[22]</sup>. Ferrites are a unique group of compounds that comprises lanthanides and fast transition metals <sup>[24]</sup>. They are magnetic oxides that have insulating nature with high saturation magnetization, permeability, low eddy current, dielectric losses, and moderate permittivity. Ferrites have a great impact on technological aspects because of their electrical and magnetic properties <sup>[25]</sup>. The application of ferrites in the technical field is based on their saturation magnetization, curie temperature, and grain size <sup>[22]</sup> high purity, chemical homogeneity, high density, and fine grain size are the important factors required for commercially important ferrites <sup>[22]</sup>. The basic properties of ferrites are based on the kind of metal atoms incorporated, their properties, and the geometric arrangement of its occupancy in the closely packed arrangement of oxygen atoms in the spiral structure <sup>[22]</sup>.

Extensive studies are done on the iron-containing transition metal oxides phases because of their unique properties viz magnetic, magnetoresistive, magneto-optical, electrical thermal, and mechanical properties. These include radiation damage resistance, high electrical resistivity and thermal conductivity, moderate thermal expansion coefficients, and energy

transfer efficiency. These properties of ferrites make them suitable as an important component of the various device, and applications that include magnetic materials such as sensors, magneto-optic sensors, catalysis, etc. They are also suitable for biotechnological applications because of their noncytotoxic nature.

Nanomaterial ferrites show different physical and chemical properties compared to their bulk counterparts because of their small size and large surface area. They are used in the field of magnetic storage, high-speed digital take, bioassay application, production of repulsive suspensions in levitated railway systems, biomolecules, ferrofluids, catalysis, and magnetic refrigeration system.

The above-mentioned properties of ferrites highly depend on dopant composition, processing conditions <sup>[26]</sup> such as synthesis method <sup>[20]</sup>, initial reactants and ion portion, pH, and thermal treatments <sup>[27]</sup>. which tunes the crystallinity, crystal size and shape, crystal size distribution, and phase purity of the resulting powdered material <sup>[26]</sup>. Particle size and morphology greatly affect the material property <sup>[28]</sup>.

The production of high purity ferrites in terms of morphology, stability, purity, and surface area is highly dependent on its synthesis method. Nanocrystals are synthesized by employing solution-based methods. Several methods are adopted for the synthesis of ferrite nanoparticles which have their own advantages and disadvantages. In the bottom-up approach, ions are combined together chemically to form tiny particles. Various synthesis techniques that come under bottom up are co-precipitation, hydrothermal, thermal decomposition, solvothermal, sol-gel, vapor deposition, micro emission, etc. In top down approach materials are brought down to tiny particles. Synthesis methods like ball milling and pulsed laser deposition come under top-down approach <sup>[29]</sup>.

#### **1.4.1 Classification of Ferrites**

Ferrites are classified on the basis of their magnetic properties and secondly by their structure.

##### **a) Classification Based on Magnetic Properties**

Ferrites are classified into soft and hard ferrites based on their magnetic coercivity and the resistance to getting demagnetized. Soft ferrites, after getting magnetized don't retain

their magnetism, whereas hard ferrites can sustain their magnetism after being magnetized and are called permanent magnets <sup>[29]</sup>.

### **1) Soft Ferrites**

Soft ferrites were first synthesized for commercial applications by Philips Research laboratories in the year 1945 though the research was started in the early 1930s. Soft ferrites are a class of ceramic electromagnetic materials which has a dark grey or black color and possess very hard and brittle properties. The name soft ferrites do not imply the physical properties of the material but represent its magnetic characteristics that do not retain significant magnetization. A class of ceramic and electromagnetic materials is generally coined by the term soft ferrites. Soft ferrites are inverse spinel and they belong to the cubic crystal. They have a homogeneous cubic spinel crystalline structure consisting of iron oxide and divalent metal oxides. Mn-Zn ( $\text{MnZnFe}_2\text{O}_4$ ) and Ni-Zn ( $\text{NiZnFe}_2\text{O}_4$ ) are the most important soft ferrites. The interactions between the metallic ions that are present in particular positions relative to the oxygen ions in the spinel crystalline structure generate magnetic domains, as per the magnetic domain theory, and this results in the magnetic properties of the ferrites. The magnetic domains are microscopically magnetized within the material. In the absence of a magnetizing force, the magnetic domains will be randomly aligned which results in the zero net flux contribution through local domains are fully magnetized. In the presence of a magnetizing force, there will be a large net flux contribution. Soft ferrites are semiconductor materials. The inherent high resistivity of ferrites results in low eddy current losses over wide frequency ranges. High magnetic permeability and stability over a wide temperature range make them better than any other electromagnetic materials. Therefore, for inductor cases, transformed losses, soft ferrites are more suitable than other magnetic materials as these are to be operated at high frequencies <sup>[29]</sup>.

### **2) Hard Ferrites**

A strong magnetization remains even after removing the applied magnetic field in hard ferrites. Even if a demagnetizing field of a certain strength is applied, the residual magnetization will be stable. They are a large class of ceramic materials that varies from dark grey to black in color and are hard and brittle. Magnetite is an example of naturally occurring weak hard ferrite. Hard ferrites will have a permanent magnetism therefore they have a major role in the permanent magnetic market. They also have high chemical stability. They have a close packing structure with oxygen and metal ions with (Fe) Iron atoms occupying the interstitial positions <sup>[29]</sup>.

Hard ferrites have a larger coercive force when compared to other metallic magnetic materials, because of which very thin magnets can be manufactured by employing them. Hard magnets are classified into two as per the orientation, viz anisotropic or oriented and isotropic or non-oriented [29].

Barium ferrite ( $\text{BaO}_6\text{Fe}_2\text{O}_3$ ) and Strontium ferrite ( $\text{SrO}_6\text{Fe}_2\text{O}_3$ ) are the most important permanent magnetic materials used for many practical purposes [29].

## b) Structural Classification of Ferrites

Ferrites are classified into four as per their crystal structure, they are:

- 1) Spinel ferrites
- 2) Garnet ferrites
- 3) Hexa ferrites
- 4) Ortho ferrites [29].

### 1) Spinel Ferrites

Spinel ferrites are a class of naturally occurring ferrites that crystallize as the cubic system [29] and have a general formula  $\text{AB}_2\text{O}_4$ , where A is a divalent cation  $\text{A}^{2+}$  and B is a trivalent cation  $\text{B}^{3+}$  [30]. Spinel ferrites are iron-containing transition metal oxide [26] so the structural formula of which can be written as  $\text{AFe}_2\text{O}_4$  where A can be Fe, Ni, Zn, Co, Mn, Mg, Cu, Cd, or a combination of these [30]. A spinel ferrite unit cell consists of 56 ions in 8 formula units i.e. 32 oxygen ions ( 8 formula units x 4 ions), 8  $\text{M}^{2+}$  ions ( 8 formula units x 1 ions), and 16  $\text{Fe}^{3+}$  ions ( 8 formula units x 2 ions). The charge on a unit cell as a whole is electrically neutral. There exist two types of crystallographic sites in the spinel structure as they are two different valence cations, the tetrahedral and the octahedral sites. The tetrahedral 'A' site is surrounded by 4 oxygen ions, called the network formers and the octahedral 'B' site is surrounded by 6 oxygen ions called the network modifiers. A spinel unit cell comprises 8 A sites and 16 B sites. Such a structure of spinel ferrites is the reason for its unique electromagnetic properties [30].



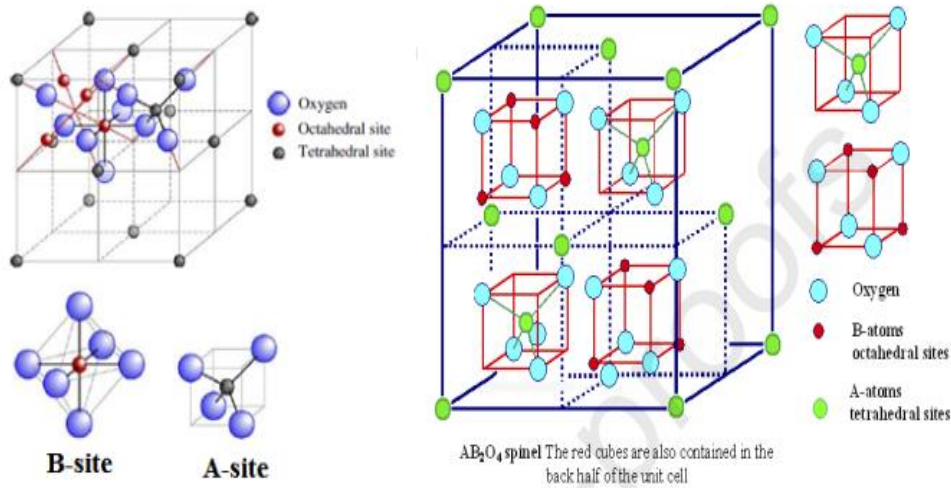


Fig 1.3(a): Spinel Ferrites <sup>[30]</sup>.

Spinel ferrites are classified according to the distribution of cations on tetrahedral ‘A’ sites and octahedral ‘B’ sites. They are:

- i) Normal Spinel ferrites
- ii) Inverse Spinel ferrites
- iii) Intermediate Spinel ferrites <sup>[30]</sup>.

**i) Normal Ferrite**

Spinel ferrites have 8 A sites that contain 8 divalent metal cations ( $M^{2+}$ ) and there are 16 B sites where all the 16 trivalent ferric ( $Fe^{3+}$ ) ions occupy. This can be represented by the formula  $(M^{2+}\downarrow)_A[Me_2^{3+\uparrow}]_BO_4^{2-}$ . The up and down arrow shows the spin directions of the A and B sites respectively. Eg  $ZnFe_2O_4$ ,  $CdFe_2O_4$  <sup>[30]</sup>.

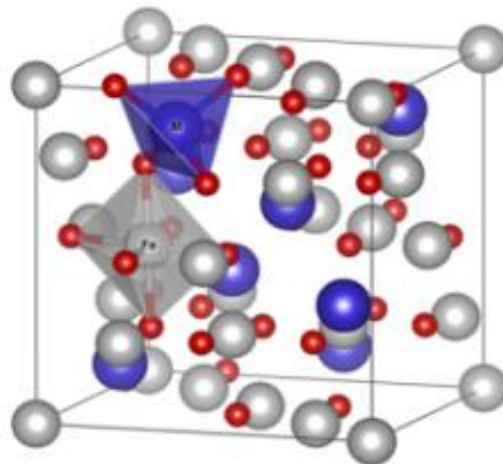


Fig 1.3(b): Normal spinel ferrite <sup>[30]</sup>.

## ii) Inverse Spinels

Spinel ferrites have 16 B sites of which 8 of them are occupied by 8 divalent metal cations. The remaining 8 B sites and the 8 A sites are occupied by the trivalent Ferric ( $\text{Fe}^{3+}$ ) ion. This can be represented by the formula  $(\text{Fe}^{3+\downarrow})_A[\text{M}^{2+\uparrow}\text{Me}^{3+\uparrow}]_B\text{O}_4^{2-}$ . The up and down arrow shows the spins of sites A and B sites respectively. Here, as the ferric ions are seen in both A and B sites they act as both network formers and network modifiers. Eg of an inverse ferrite is  $\text{Fe}_3\text{O}_4$  [30].

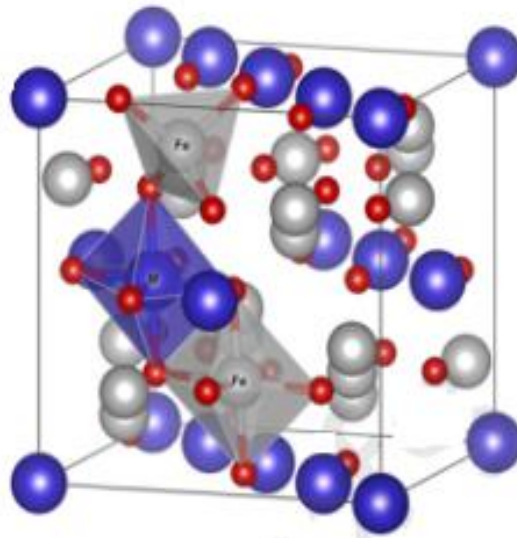


Fig 1.3 (c): Inverse spinel ferrite [30].

## iii) Intermediate Spinel ferrites

The ionic distribution in intermediate spinel ferrites lies between normal and inverse and it is called intermediate or random or mixed spinel ferrite [31]. This distribution can be represented by the formula:



where  $\delta=1$  for normal spinel ferrite,  $\delta=0$  for complete inverse spinel ferrite [31].

the  $\delta$  ranges between 1 and 0 for the intermediate spinel ferrites.  $\delta=1/3$  for a complete random spinel ferrite. As the name implies, a mixed ferrite will consist of an unequal number of cations on octahedral sites. Eg for this type of ferrites are  $\text{MgFe}_2\text{O}_4$  and  $\text{MnFe}_2\text{O}_4$  [31].

M represents divalent ions and Me represents trivalent ions. The parenthesis is generally used to represent tetrahedral and octahedral sites are represented in the square brackets [31].

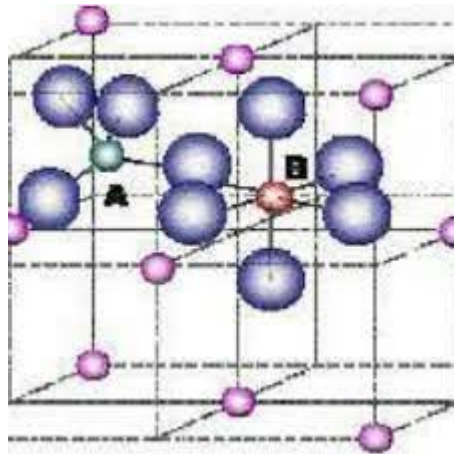


Fig1.3 (d): Intermediate Spinel Ferrite <sup>[32]</sup>.

## 2) Garnet Ferrites

Garnet ferrites consist of trivalent rare earth elements of large magnetic moments, they crystallize in the dodecahedral structure to the mineral garnet. The general formula of garnet ferrite can be written as  $Me_3Fe_5O_{12}$ . The specialty of garnet ferrites is that all the metal ions in the structure are trivalent <sup>[29]</sup>. They have a total of 8 formula units and 3 sub lattices.  $Fe^{3+}$  ions occupy octahedral and tetrahedral sites in the ratio of 2:3 and the trivalent metal ions occupy diode octahedral sites <sup>[33]</sup>. Garnet ferrites are highly suitable due to the full occupancy of sites by cations <sup>[29]</sup>. Eg of a garnet ferrite is  $Y_3Fe_5O_{12}$  which shows ferrimagnetic behavior <sup>[33]</sup>.

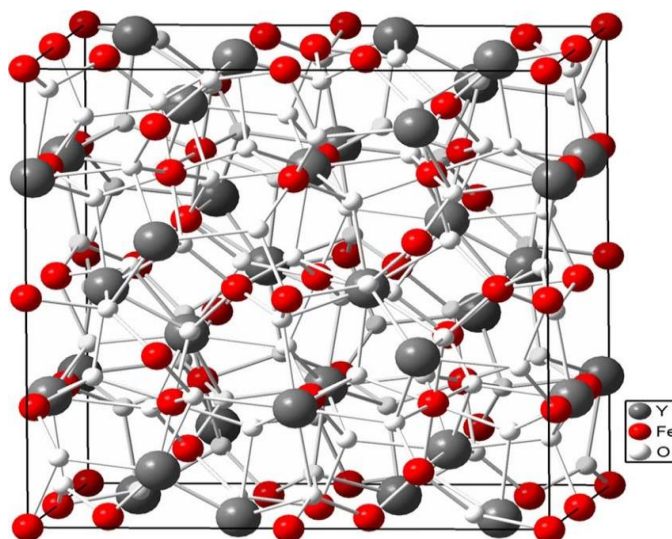


Fig1.4: Garnet Ferrite <sup>[34]</sup>.

### 3) Hexagonal Ferrites

Hexagonal ferrites also known as hexaferrite, have tremendous growth nowadays. They are now inevitable materials in the field of commerce and technology because of their multitude of uses and applications. They are used as permanent magnets, magnetic recovering, and data storage, and also used as components in various electrical devices [35].

Hexagonal ferrites have a highly complex structure. The general formula can be written as  $\text{MeF}_{12}\text{O}_{19}$  where Me can be Ba, Sr or Pb. They are further classified as M, W, T,, Z and U ferrites [35].

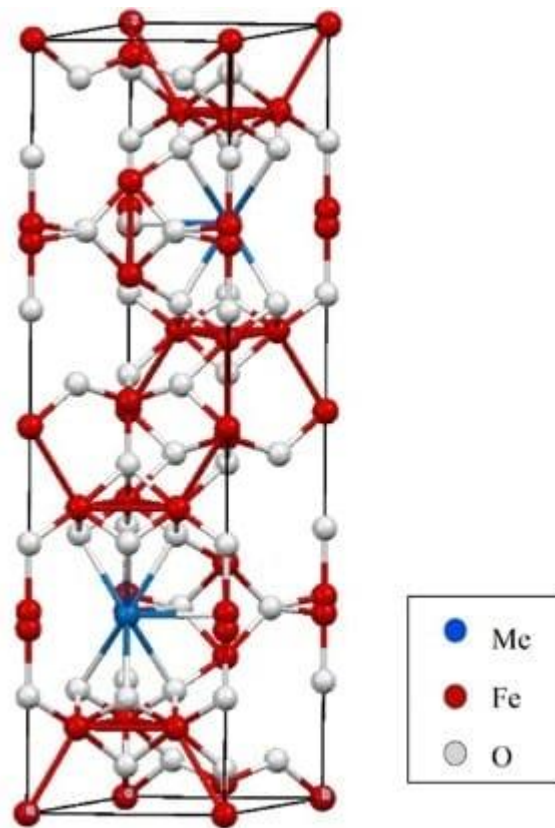


Fig 1.5: Hexagonal ferrites [36].

### 4) Ortho Ferrites

Ortho ferrites are also cubic ferrites with a slightly distorted and perovskite structure. The term perovskite is defined as the atomic arrangement of oxides in the  $\text{RMO}_3$  structure. Materials that have cubic symmetry and a complicated molecular arrangement will have this structure. Orthoferrites are widely used as bubble memory structures [29].

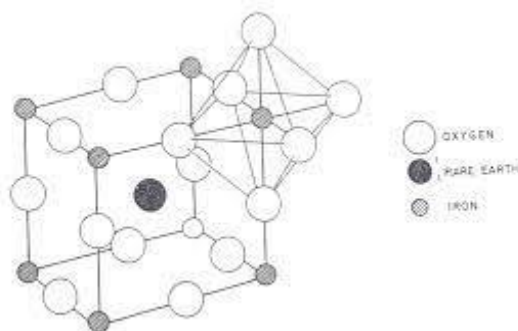


Fig 1.6: Ortho ferrites <sup>[37]</sup>.

### 1.4.2 Spinel Ferrites as Adsorbents

The introduction of magnetic nanoparticles as a solution for environmental issues has become a breakthrough. Spinel ferrites have been used as a new class of adsorbent material for cleaning drinking water and wastewater management. Ferrites are an excellent class of pollutant removal through magnetic-assisted chemical separation. High surface area, adjustable morphology, ease of functionalization, and the superparamagnetic nature aids for its attractive efficiency in the removal of several pollutants in both batch or continuous system without generating secondary wastes thus by ensuring high economic as well as environmental potency<sup>[38]</sup>.

Magnetite is the chief component of ferrites due to its high saturate magnetization. The ferrite  $\text{Fe}_3\text{O}_4$  oxidizes into iron oxide as per the environment conditions and this affects its magnetic properties thus by influencing the efficiency of the chemical separation<sup>[38]</sup>.

Ferrite-based nanoparticles with a general formula  $\text{MFe}_2\text{O}_4$ ,  $\text{M} = \text{Mg, Mn, Co, Ni, Zn}$ , have an appreciable performance. They have higher chemical resistance and strong magnetic features when compared to magnetite <sup>[38]</sup>. The type of cation and their distribution on the sites in the crystal structure can be tuned because of which they show astonishing properties <sup>[39]</sup>.

The magnetic nature of the spinel ferrite nanoparticles i.e. the superparamagnetic behavior at their nanometer size aids in the ability to remove them from a solution on the application of an external magnetic field <sup>[19]</sup>.

Spinel ferrites are economical and they are also environmentally friendly because of which studies in this particular area are so vast. Spinel ferrites can be made with spinel

ferrites with tuneable size and shape, large surface-to-volume ratio, and appreciable magnetic property resulting in them being a long-lasting and efficient adsorbent material [40].

Zinc ferrite is a normal spinel structure with  $Zn^{2+}$  occupies tetrahedral sites and  $Fe^{3+}$  in the octahedral sites [41]. Bulk zinc ferrite with this structure, the tetrahedral sites are occupied with  $Zn^{2+}$  ions without magnetic moment and hence it is anti-ferromagnetic. The magnetic properties of nanocrystalline zinc ferrites can be influenced by the crystallite size and synthesis method. The reduction of iron and zinc cations in the octahedral and tetrahedral sites tunes its magnetic nature and tunes into ferrimagnetic [21].

Zinc substitution on ferrites has a crucial role in tuning the magnetic properties of a nanoscale system [40]. Zinc ferrites have a variety of wide applications because of their anti-ferromagnetic and superparamagnetic behavior.  $ZnFe_2O_4$  has a high specific capacity calculated theoretically when compared to  $Fe_3O_4$  hence it is much apt for higher energy density applications [27].

Zinc ferrites are in the spotlight in vast research because of the preference of the zinc ion to occupy the tetrahedral site in the spinel structure. This results in a simpler magnetic system for study. Such a structure is preferred to understand the location of cations, the magnitude of atomic movements, their orientation and interaction [42].

There are a number of methods for the synthesis of Zinc ferrite nanoparticles. They are co-precipitation, radio frequency sputtering, sol-gel, and hydrothermal synthesis [42]. By employing the co-precipitation method, ultra-fine ferrite particle formation is ensured [43]. The parameters viz the initial reactants, their composition, pH, temperature conditions, and the synthesis procedure will influence crystallinity, morphology, and magnetism [27].

Zinc ferrite nanoparticles show excellent electrical, optical, and magnetic properties as per their size, shape, and composition. These properties make  $ZnFe_2O_4$  stand out from other spinel nanoparticles [44]. Zinc ferrite nanoparticles have a unique thermal and chemical stability and lower toxicity when compared to other ferrites [45].

Nizam, Thanooja et al [16] studied the removal of Cr (VI) ions from an aqueous solution by employing sol-gel derived Ni, Zn, and Cu ferrites and showed that  $ZnFe_2O_4$  was the most efficient metal ferrite among others. This enhanced adsorption capacity promised by zinc ferrite is influenced by the content of zinc in it and also by its site occupation in the crystal structure [46].

Various synthesis procedures are employed for the synthesis of nanomaterials and this includes both physical and chemical methods<sup>[47]</sup>, still, the stability of such synthesized nanoparticles and the chemicals that are used in the synthesis procedure will be toxic which are used for metal reduction and for particle stabilization. As a result, the chemically synthesized nanoparticles will have functional groups which are much active and they may cause harm to biological systems because of their toxic nature<sup>[48]</sup>. The physical method requires conditions of high temperature pressure and other external forces for breaking down the material to the nano range. So, the toxic by-products that are produced as a result of employing these conventional methods are a threat to the environment and its beings. Moreover, the chemical solvents that are employed in the synthesis procedure make the extraction of the nanoparticles difficult. These problems are an obstruction in the field of using it for medical applications<sup>[49]</sup>.

Biosynthesis is of great attraction in the research field as its non-toxic, cost-effective, and environmentally friendly. Moreover, Biosynthesised nanoparticles have primarily physiochemical characteristics such as a large surface-to-volume ratio, better optical properties, and stable, surface functionalization<sup>[50]</sup>. Bio route of synthesis method offers an economical, environment-friendly procedure that does not require high temperature and pressure conditions without the use of toxic chemicals. Nanoparticles synthesized in such a manner will be biocompatible because of the use of bio residues which are usually plant extracts. These nanoparticles show less toxicity because of their natural origin and can be exposed to either body or bodily fluids. Properties such as less toxicity, bioavailability, and appreciable magnetic nature make them capable to get included in biomedical applications. As the surface of biologically synthesized nanomaterials is coated with non-toxic biomolecules, they will be biocompatible, and this coating also ensures stability, and thus metallic nanoparticles are not that easily oxidized in the presence of water and oxygen and this attributes to their capability to include it in biological applications. The surface hydroxyl groups present in the biomolecules act as the capping agents and form coating on the magnetic nanoparticles<sup>[45]</sup>. This also enhances the solubility and stability of the nanoparticles under a wide range of conditions<sup>[50]</sup>.

The Green route makes use of any plant part, fungi, algae, bacteria, or the whole plant itself as the source of biomolecules<sup>[50]</sup>. A major advantage of green synthesis includes its simplicity in the procedure, high yield, low toxicity, low cost, and control over size by controlling the parameters viz pH and temperature. As the biomolecules act as the stabilizers,

there is no need of using additional stabilizers to prevent aggregation [47]. The chemical, physical and optical properties influence the morphological structure of nanoparticles [51].

The bio method of synthesis technique of nanomaterials employs a bottom-up approach involving the redox process of metal ions and stabilizing process in which the size regulation is done and the nanoparticles agglomerate. The three important steps for biosynthesis are: [52]

- i) The selection of reaction medium solvent
- ii) A correct eco-friendly reducing agent
- iii) A non-toxic stabilizing agent as a capping agent [52].

The plant mediate mediated synthesis can be either intercellular. As the name suggests, the intercellular synthesis occurs inside the plant whereas the latter occurs invitro, of which extracellular plant-mediated synthesis is better than the intra-cellular plant-mediated synthesis [53].

## **1.5 NANOMATERIALS IN WASTEWATER TREATMENT**

The growing demand for water and the scarcity of its source seeks attraction for researchers to find an ultimate solution for developing a sustainable water treatment method that results in obtaining safe and clean drinking water

Adsorption of various pollutants through nanoparticles ensures economic and environmental benefits will be beneficial. Ideal adsorption systems are which can remove even slowly biodegradable or nonbio debiodegradable synthetic compounds. The presence of biomolecules on the surface of the nanoparticle enhances the number of adsorption sights thereby escalating the efficiency of the removal of pollutants [54].

## **1.6 PROJECT OUTLINE**

Waste water management is a serious issue of all time. All industrial process including agricultural, tanning, planting, and metal processing results in polluting the water due to an increase in the concentration of heavy metals. Here in the present work, adsorption is chosen for the removal studies of Zinc ferrite nanoparticles

Chemically synthesized nanomaterials have proved their efficiency in heavy metal removal and this is evident from the literature review. Nizam, Thanooja et al have studied the adsorption studies of Chromium (Sol-gel derivative) Metal ferrites  $MFe_2O_4$  (M= Ni, Cu, Zn)



and optimized the parameters that affect the adsorption process. It was found that zinc ferrites were the most efficient among the others.

The present work is an attempt to investigate how the synthesis method plays a role in the adsorptive property of ZnFe<sub>2</sub>O<sub>4</sub> nanoparticles. In this regard, a comparative study of the adsorptive property of both chemical and bio-synthesized ZnFe<sub>2</sub>O<sub>4</sub> is conducted. For this, the optimized values of the previous study<sup>[16]</sup> are taken as the reference. The experimental details and the results are discussed in the following chapters.

## 1.7 LITERATURE REVIEW

S. Hafez Ghoran et al synthesized ZnFe<sub>2</sub>O<sub>4</sub> nanoparticles using hydroethanolic extract of *Citrus aurantium* flowers. The biomolecules present in the plant extract act as the stabilizing agent for the synthesized nanoparticles and offered better morphology and reduced crystallite size. Pure ZnFe<sub>2</sub>O<sub>4</sub> nanoparticles with a non-toxic coating were achieved.<sup>[45]</sup>

M. I. Din et al synthesized ZnFe<sub>2</sub>O<sub>4</sub> nanoparticles using aqueous extract of *Piper nigrum* seeds. Ultra-pure ZnFe<sub>2</sub>O<sub>4</sub> sample with a size range 60-80nm was obtained. The photocatalytic reduction of as-synthesized ZnFe<sub>2</sub>O<sub>4</sub> nanoparticles towards methylene blue was studied. The factors responsible for the degradation phenomenon were also studied.<sup>[55]</sup>

L. W. Yeary et al studied the microbial synthesis of ZnFe<sub>2</sub>O<sub>4</sub> nanoparticles using the metal-reducing bacterium *Thermoanaerobacter*. The crystallite size, lattice parameters, and magnetic properties of the synthesized sample were studied and verified with previously reported literature.<sup>[42]</sup>

V. A. Fabiani et al synthesized ZnFe<sub>2</sub>O<sub>4</sub> nanoparticles using *Antidesma bunius* L fruit extract with Zn to Fe precursor ratio 1:2 via co-precipitation method and studied the characteristics by varying the calcination temperature. The formation of pure spinel ZnFe<sub>2</sub>O<sub>4</sub> nanoparticles was confirmed by employing characterization techniques.<sup>[56]</sup>

Mohana Sriramulu et al synthesized ZnFe<sub>2</sub>O<sub>4</sub> nanoparticles using *Aegle marmelos* leaves extract. The structural and morphological characteristics of the as-synthesized nanoparticles were studied. The applicability of the synthesized nano ferrites towards antibacterial activity and drug delivery was examined.<sup>[44]</sup>

Manish Kumar et al reviewed recent studies in the last two decades in the area of health hazards caused due to the consumption of heavy metals through water and their removal

using magnetic nano ferrites and their derivatives. They also discuss the sources and effects of heavy metals in the environment.<sup>[1]</sup>

Nizam Thanooja et al synthesized nano metal ferrites  $MFe_2O_4$ , ( $M = Ni, Zn, Cu$ ) via sol-gel method and studied comparative adsorption efficiency on the removal of  $Cr^{6+}$  ions from the prepared synthetic wastewater. The factors affecting the adsorption process such as pH, temperature, contact time, adsorbate concentration, and adsorbent dosage were studied from batch adsorption studies. They reported that  $ZnFe_2O_4$  showed the highest adsorption efficiency.<sup>[16]</sup>

G.A.V. Magalhaes-Ghiotto ~ et al. reported a review of research trends on green nanoparticles in water treatment. They also studied their applications, environmental aspects, and large-scale production. The use of nanoparticles in water treatment and commonly occurring problems are discussed in the review.<sup>[54]</sup>

A. Kaur et al. synthesized Iron hydroxide,  $Fe(OH)_3$ , from aqueous extract of *Acacia catechu* leaves.  $Fe(OH)_3$  was annealed and highly crystalline  $\alpha-Fe_2O_3$  nanoparticles were formed. The crystallite size, porosity, size and shape of the prepared samples were investigated. The adsorptive removal of  $Cr^{6+}$  ions by varying pH, adsorbent dosage and initial ion concentration were studied. They reported that the presence of surface hydroxyl groups has a major role in the adsorptive properties of the ferrite samples<sup>[57]</sup>.

H. Muthukumar et al synthesized  $AgFeO_2$  nanoparticles using *Amaranthus blitum* leaves extract. They compared the properties of biologically synthesized  $AgFeO_2$  and chemically synthesized  $AgFeO_2$  nanoparticles. They conclude that biosynthesis offers nanoparticles with reduced size, better morphology, less toxicity, and better surface area<sup>[58]</sup>.

## REFERENCES

- 1) Bharti, Manish Kumar, et al. "Potential of magnetic nanoferrites in removal of heavy metals from contaminated water: mini review." *Journal of Superconductivity and Novel Magnetism* 33.12 (2020): 3651-3665.
- 2) <https://www.veluda.com/en/blog/15-endaferon-dedomena-gia-ti-molunsi-tou-nerou-220>
- 3) Duruibe, J. Ogwuegbu, M. O. C. Ogwuegbu, and J. N. Ekwurugwu. "Heavy metal pollution and human biotoxic effects." *International Journal of physical sciences* 2.5 (2007): 112-118.
- 4) Tseng, Chao-Heng, Chieh Lei, and Ying-Chu Chen. "Evaluating the health costs of oral hexavalent chromium exposure from water pollution: a case study in Taiwan." *Journal of Cleaner Production* 172 (2018): 819-826.
- 5) Saha, Priti, and Biswajit Paul. "Assessment of heavy metal pollution in water resources and their impacts: A review." *J. Basic Appl. Eng. Res* 3 (2016): 671-675.
- 6) Rengaraj, S., Kyeong-Ho Yeon, and Seung-Hyeon Moon. "Removal of chromium from water and wastewater by ion exchange resins." *Journal of hazardous materials* 87.1-3 (2001): 273-287.
- 7) Dotaniya, M. L., et al. "Chromium pollution: a threat to environment-a review." *Agricultural Reviews* 35.2 (2014).
- 8) Kimbrough, David Eugene, et al. "A critical assessment of chromium in the environment." *Critical reviews in environmental science and technology* 29.1 (1999): 1-46.
- 9) Jabłońska-Czapla, Magdalena. "Arsenic, antimony, chromium, and thallium speciation in water and sediment samples with the LC-ICP-MS technique." *International journal of analytical chemistry* 2015 (2015).
- 10) World Health Organization. *Chromium in drinking-water*. No. WHO/HEP/ECH/WSH/2020.3. World Health Organization, 2020.
- 11) Hubicki, Zbigniew, and Dorota Kołodyńska. "Selective removal of heavy metal ions from waters and waste waters using ion exchange methods." *Ion exchange technologies* 7 (2012): 193-240.

- 12) Polat, Hurriyet, and D. Erdogan. "Heavy metal removal from waste waters by ion flotation." *Journal of Hazardous Materials* 148.1-2 (2007): 267-273.
- 13) Bakalár, Tomáš, Milan Búgel, and Lucia Gajdošová. "Heavy metal removal using reverse osmosis." *Acta Montanistica Slovaca* 14.3 (2009): 250.
- 14) Gunatilake, S. K. "Methods of removing heavy metals from industrial wastewater." *Methods* 1.1 (2015): 14.
- 15) Qasem, Naef AA, Ramy H. Mohammed, and Dahiru U. Lawal. "Removal of heavy metal ions from wastewater: A comprehensive and critical review." *Npj Clean Water* 4.1 (2021): 1-15.
- 16) Nizam, Thanooja, et al. "Adsorption efficiency of sol–gel derived nano metal ferrites, MFe<sub>2</sub>O<sub>4</sub> (M= Ni, Zn, Cu) on the removal of Cr (VI) ions from aqueous solution." *Journal of Sol-Gel Science and Technology* 101.3 (2022): 618-629.
- 17) Grassi, Mariangela, et al. "Removal of emerging contaminants from water and wastewater by adsorption process." *Emerging compounds removal from wastewater*. Springer, Dordrecht, 2012. 15-37.
- 18) Kecili, Rustem, and Chaudhery Mustansar Hussain. "Mechanism of adsorption on nanomaterials." *Nanomaterials in Chromatography*. Elsevier, 2018. 89-115.
- 19) Kefeni, Kebede K., Bhekie B. Mamba, and Titus AM Msagati. "Application of spinel ferrite nanoparticles in water and wastewater treatment: a review." *Separation and Purification Technology* 188 (2017): 399-422.
- 20) Korotkova, A. M., et al. "Green synthesis of zinc based nanoparticles zinc ferrite by *Petroselinum crispum*." *IOP Conference Series: Earth and Environmental Science*. Vol. 341. No. 1. IOP Publishing, 2019.
- 21) Shahraki, R. Raeisi, et al. "Structural characterization and magnetic properties of superparamagnetic zinc ferrite nanoparticles synthesized by the coprecipitation method." *Journal of Magnetism and Magnetic Materials* 324.22 (2012): 3762-3765.
- 22) [http://ir.unishivaji.ac.in:8080/jspui/bitstream/123456789/1847/8/08\\_Chapter%201.pdf](http://ir.unishivaji.ac.in:8080/jspui/bitstream/123456789/1847/8/08_Chapter%201.pdf)
- 23) [https://www.researchgate.net/profile/Carlos-Arean/post/What the types of ferrites/attachment/59d6501b79197b80779a90f6/AS%3A501196488011776%401496505962673/download/Ferrites++1.pdf](https://www.researchgate.net/profile/Carlos-Arean/post/What%20the%20types%20of%20ferrites/attachment/59d6501b79197b80779a90f6/AS%3A501196488011776%401496505962673/download/Ferrites++1.pdf)

- 24) Srivastava, Richa, and Bal Chandra Yadav. "Ferrite materials: introduction, synthesis techniques, and applications as sensors." *International Journal of Green Nanotechnology* 4.2 (2012): 141-154.
- 25) [https://shodhganga.inflibnet.ac.in/bitstream/10603/13720/7/07\\_chapter%201.pdf](https://shodhganga.inflibnet.ac.in/bitstream/10603/13720/7/07_chapter%201.pdf)
- 26) Gatelytè, Aurelija, et al. "Sol-gel synthesis and characterization of selected transition metal nano-ferrites." *Materials science* 17.3 (2011): 302-307.
- 27) Almessiere, M. A., et al. "Biosynthesis effect of Moringa oleifera leaf extract on structural and magnetic properties of Zn doped Ca-Mg nano-spinel ferrites." *Arabian Journal of Chemistry* 14.8 (2021): 103261.
- 28) Thomas, Marykutty, and K. C. George. "Infrared and magnetic study of nanophase zinc ferrite." (2009).
- 29) Shaikh, Shoyebmohamad F., et al. "Types, synthesis methods and applications of ferrites." *Spinel Ferrite Nanostructures for Energy Storage Devices*. Elsevier, 2020. 51-82.
- 30) Narang, Sukhleen Bindra, and Kunal Pubby. "Nickel spinel ferrites: a review." *Journal of Magnetism and Magnetic Materials* 519 (2021): 167163.
- 31) Thakur, Leena, and Brijesh Singh. "History and applications of important ferrites." *Integrated Research Advances* 1.1 (2014): 11-13.
- 32) Sharma, J. K., et al. "Nanoferrites of transition metals and their catalytic activity." *Solid State Phenomena*. Vol. 241. Trans Tech Publications Ltd, 2016.
- 33) Mallmann, E. J. J., et al. "Yttrium iron garnet: properties and applications review." *Solid State Phenomena*. Vol. 202. Trans Tech Publications Ltd, 2013.
- 34) Harris, Vincent G. "Modern microwave ferrites." *IEEE Transactions on Magnetism* 48.3 (2011): 1075-1104.
- 35) Pullar, Robert C. "Hexagonal ferrites: a review of the synthesis, properties and applications of hexaferrite ceramics." *Progress in Materials Science* 57.7 (2012): 1191-1334.
- 36) Mei, Liu, Atsushi Iizuka, and Etsuro Shibata. "Recent progress on utilization of metal-rich wastes in ferrite processing: a review." *Waste and Biomass Valorization* 9.9 (2018): 1669-1679.
- 37) Usman, Ibrahim Bala. *Synthesis and Characterization of Sm-based Orthoferrite Compounds, SmFe<sub>1-x</sub>Mn<sub>x</sub>O<sub>3</sub>*. Diss. University of the Witwatersrand, 2010.

- 38) Da Silva, F. G., et al. "Structural and magnetic properties of spinel ferrite nanoparticles." *Journal of nanoscience and nanotechnology* 19.8 (2019): 4888-4902.
- 39) Kurian, Manju, and Divya S. Nair. "Effect of preparation conditions on nickel zinc ferrite nanoparticles: a comparison between sol–gel auto combustion and co-precipitation methods." *Journal of Saudi Chemical Society* 20 (2016): S517-S522.
- 40) Reddy, D. Harikishore Kumar, and Yeoung-Sang Yun. "Spinel ferrite magnetic adsorbents: alternative future materials for water purification?." *Coordination Chemistry Reviews* 315 (2016): 90-111.
- 41) Jeseentharani, V., et al. "Synthesis of metal ferrite (MFe<sub>2</sub>O<sub>4</sub>, M= Co, Cu, Mg, Ni, Zn) nanoparticles as humidity sensor materials." *Journal of experimental nanoscience* 8.3 (2013): 358-370.
- 42) Yeary, Lucas W., et al. "Magnetic properties of bio-synthesized zinc ferrite nanoparticles." *Journal of Magnetism and Magnetic Materials* 323.23 (2011): 3043-3048.
- 43) Arulmurugan, R., et al. "Effect of zinc substitution on Co–Zn and Mn–Zn ferrite nanoparticles prepared by co-precipitation." *Journal of Magnetism and Magnetic Materials* 288 (2005): 470-477.
- 44) Sriramulu, Mohana, Dhananjay Shukla, and Shanmugam Sumathi. "Aegle marmelos leaves extract mediated synthesis of zinc ferrite: antibacterial activity and drug delivery." *Materials Research Express* 5.11 (2018): 115404.
- 45) Hafez Ghoran, Salar, et al. "Biosynthesis of zinc ferrite nanoparticles using polyphenol-rich extract of Citrus aurantium flowers." *Nanomedicine Research Journal* 5.1 (2020): 20-28.
- 46) Wu, Can, et al. "Enhanced adsorption of arsenate by spinel zinc ferrite nanoparticles: Effect of zinc content and site occupation." *Journal of Environmental Sciences* 79 (2019): 248-255.
- 47) Rai, Mahendra, and Clemens Posten, eds. *Green biosynthesis of nanoparticles: mechanisms and applications*. CABI, 2013.
- 48) Arokiyaraj, Selvaraj, et al. "Green Synthesis of Metallic Nanoparticles Using Plant Compounds and Their Applications: Metallic Nanoparticles Synthesis Using Plants." *Emerging Research on Bioinspired Materials Engineering*. IGI Global, 2016. 1-34.

- 49) Lee, Kar Xin, et al. "Recent developments in the facile bio-synthesis of gold nanoparticles (AuNPs) and their biomedical applications." *International journal of nanomedicine* 15 (2020): 275.
- 50) Ali, Salman, et al. "State of the art of gold (Au) nanoparticles synthesis via green routes and applications: A review." *Environmental Nanotechnology, Monitoring & Management* 16 (2021): 100511.
- 51) Ahmed, Shakeel, Saif Ali Chaudhry, and Saiqa Ikram. "A review on biogenic synthesis of ZnO nanoparticles using plant extracts and microbes: a prospect towards green chemistry." *Journal of Photochemistry and Photobiology B: Biology* 166 (2017): 272-284.
- 52) de Jesus, Roberta Anjos, et al. "Environmental remediation potentialities of metal and metal oxide nanoparticles: mechanistic biosynthesis, influencing factors, and application standpoint." *Environmental Technology & Innovation* 24 (2021): 101851.
- 53) Khatoon, Nafeesa, Jahirul Ahmed Mazumder, and Meryam Sardar. "Biotechnological applications of green synthesized silver nanoparticles." *J. Nanosci. Curr. Res* 2.107 (2017): 2572-0813.
- 54) Magalhães-Ghiotto, Grace AV, et al. "Green nanoparticles in water treatment: a review of research trends, applications, environmental aspects and large-scale production." *Environmental Nanotechnology, Monitoring & Management* 16 (2021): 100526.
- 55) Din, Muhammad Imran, et al. "Green synthesis of zinc ferrite nanoparticles for photocatalysis of methylene blue." *International Journal of Phytoremediation* 22.13 (2020): 1440-1447.
- 56) Fabiani, V. A., F. I. P. Sari, and S. A. Putri. "Biosynthesis and characterization of zinc ferrite (ZnFe<sub>2</sub>O<sub>4</sub>) via *Antidesma bunius* L. fruit extract." *IOP Conference Series: Earth and Environmental Science*. Vol. 926. No. 1. IOP Publishing, 2021.
- 57) Kaur, Amrit, et al. "Sustainable preparation of Fe (OH)<sub>3</sub> and α-Fe<sub>2</sub>O<sub>3</sub> nanoparticles employing *Acacia catechu* extract for efficient removal of chromium (VI) from aqueous solution." *Environmental Nanotechnology, Monitoring & Management* 16 (2021): 100593.
- 58) Muthukumar, Harshiny, et al. "Plant extract mediated synthesis enhanced the functional properties of silver ferrite nanoparticles over chemical mediated synthesis." *Biotechnology Reports* 26 (2020): e00469.

# CHAPTER 2

## EXPERIMENTAL TECHNIQUES

### 2.1 SYNTHESIS METHOD: CO-PRECIPIATION METHOD

Co-precipitation is an economically feasible method for the synthesis of spinel ferrites at low temperatures and also often without calcination at higher temperatures<sup>[1][2]</sup>. It is a simple and cost-effective technique making use of which the size and size distribution can be controlled by regulating the relative rates of nucleation and growth process during the synthesis procedure<sup>[3]</sup>.

Co-precipitation is defined as the metal adsorption on the surface of the precipitate or the incorporation of the metal ions on the surface of the precipitate. The precipitation process is followed by the removal of the precipitate by centrifugation and filtration<sup>[4]</sup>.

The three principal mechanisms involved in a co-precipitation process are surface adsorption, where the ions in the solution are attracted by the surface charge on the precipitate; inclusion, where the analyte is incorporated in the crystal structures of the precipitate isomorphically or non isomorphically; occlusion in which, before getting dispersed, the precipitate traps the ions<sup>[4]</sup>.

When direct precipitation cannot obtain metallic species because of its lower concentration in the sample solution, co-precipitation is used and this is the apt method for the preparation of ultrafine spinel ferrite nanoparticles. For ensuring nanoparticles of high crystallinity, homogeneity, and fine textural properties, co-precipitation is employed with a constant pH<sup>[5]</sup>. The solid precursors are a homogenous mixture of cations that can be solid or a mixture of cations that can be solid or a mixture of multiple salts. The nuclei formed during the process grow uniformly to form a homogenous nanocrystalline powder. The prepared insoluble sample solution which is a mixture of cations is heated for decomposition and transformation to the required metal oxides<sup>[6]</sup>.

As Co-precipitation promises the production of homogenous particles, it is often used as an ideal method for the synthesis of nano ferrites on a bulk scale. Ultrafine metal substituted ferrite nanoparticles are assured by employing this method<sup>[7]</sup>. Co-precipitation is an



attractive synthesis technique as it assures homogeneity, contamination-free, and provision to control the particle size of the synthesized spinel ferrite nanoparticle<sup>[1]</sup>.

## 2.1.1 SYNTHESIS PROCEDURE

### i) Materials

Ferric Nitrate  $\text{Fe}(\text{NO}_3)_3 \cdot 9\text{H}_2\text{O}$  (98%), Zinc Nitrate Hexa hydrate  $\text{Zn}(\text{NO}_3)_2 \cdot 6\text{H}_2\text{O}$  (96%), and Ammonium Hydroxide (25%) were obtained from Nice Chemicals Pvt Ltd. All chemicals were used without further purification. Ultrapure water was obtained from the Bransted E-Pure deionization system.

### i) Methods

The preparation of Zinc Ferrite nanoparticles was done by adopting the co-precipitation method. The extract of *Zingiber officinale* was used in the process.

### ii) Preparation of Plant Extracts

The plant part was collected and dissolved in a known amount of distilled water and magnetically stirred at 60°C. The acquired color filtrate was stored in an airtight glass bottle and was kept in the refrigerator.

### iii) Preparation of Zinc Ferrite Nanoparticles

Zinc-doped magnetic nanoparticles were prepared by employing the co-precipitation method using an aqueous extract of *Zingiber officinale*. Zinc Nitrate Hexahydrate  $\text{Zn}(\text{NO}_3)_2 \cdot 6\text{H}_2\text{O}$  and Ferric Nitrate  $\text{Fe}(\text{NO}_3)_3 \cdot 9\text{H}_2\text{O}$  were taken in the ratio of 1:2. The precursor solution was mixed together. This mixture and the plant extract were added dropwise simultaneously to a beaker with distilled water. This process was followed by making the pH environment of the solution basic. The solution was magnetically stirred for 6 hours and kept overnight for it to settle down. The sample solution is then centrifuged with distilled water several times till the pH becomes neutral and then it is filtered using Whatmann filter paper. The contents in the filter paper are collected on a petri dish and dried at 80°C and then powdered using agate mortar and pestle. The *Zingiber officinale* mediated synthesized sample was named "C". The XRD pattern of sample C was noted before calcination. The sample was calcined at 100°C, 200°C, 300°C, and 400°C, and XRD were taken for each set to optimize the calcination temperature.

The synthesized samples were studied by undergoing characterization techniques viz X-Ray Diffraction (XRD), Fourier Transform Infrared Spectroscopy (FTIR).

## 2.2 PREPARATION OF SYNTHETIC WASTEWATER

Stoichiometric amounts of Potassium Dichromate ( $K_2Cr_2O_7$ ) were weighed and dissolved in distilled water to obtain the stock solutions of desired concentrations of  $Cr^{6+}$ .

One part per million is defined as one part of the solute per one million parts solvent or  $10^{-6}$ . The measurement of the relative abundance of a solute that is dissolved in water implies that 1 ppm is the amount of solute in mg dissolved in 1Kg of water and as the density of water is 1Kg/L, it is equivalent to the solute weighed in mg dissolved in 1L of water.

The Formula weight of  $K_2Cr_2O_7 = 294.185$

Atomic Weight of Chromium = 51.9961

There are two atoms in one formula unit of  $K_2Cr_2O_7$

i.e., there are  $(2 \times 51.9961)g = 103.9922g$  of Cr(VI) present in 294.185g of  $K_2Cr_2O_7$ .

Amount of  $K_2Cr_2O_7$  that contain 1g of Cr =  $\frac{1 \times 294.185}{2 \times 51.9961} = 2.8289g$

A 1000ppm Cr(VI) solution is obtained by dissolving 2.8289g of  $K_2Cr_2O_7$  in 1L of water.

For convenience, we can also prepare a 1000 ppm solution by taking 0.28289g of  $K_2Cr_2O_7$  in 100mL of water.

Stock solutions of lower concentrations can be obtained by applying the dilution formula:

$$C_1V_1 = C_2V_2$$

Where  $C_1$  = initial concentration

$C_2$  = final concentration

$V_1$  = initial volume

$V_2$  = final volume

**i) Preparation of 100ppm Cr(VI) solution from 1000ppm Cr(VI) solution**

$$C_1 = 1000 \text{ ppm}$$

$$C_2 = 100 \text{ ppm}$$

$$V_2 = 200 \text{ mL}$$

$$V_1 = \frac{C_2 V_2}{C_1} = \frac{200 \times 100}{1000} = 20 \text{ mL}$$

So by making up 20mL of 1000ppm Cr (VI) solution to 200mL, we get 100 ppm Cr (VI) solution.

**ii) Preparation of 25 ppm Cr(VI) solution from 100 ppm Cr(VI) solution**

$$C_1 = 100 \text{ ppm}$$

$$C_2 = 25 \text{ ppm}$$

$$V_2 = 200 \text{ mL}$$

$$V_1 = \frac{C_2 V_2}{C_1} = \frac{25 \times 200}{100} = 50 \text{ mL}$$

50mL of 100 ppm Cr(VI) solution is made up to 200 mL, and 25 ppm Cr(VI) solution is obtained.

**iii) Preparation of 10ppm Cr(VI) solution from 25 ppm Cr(VI) solution**

$$C_1 = 25 \text{ ppm}$$

$$C_2 = 10 \text{ ppm}$$

$$V_2 = 50 \text{ mL}$$

$$V_1 = \frac{C_2 V_2}{C_1} = \frac{10 \times 50}{25} = 20 \text{ mL}$$

20mL of 25 ppm Cr(VI) solution is made up to 50 mL, and 10 ppm Cr(VI) solution is obtained.

## **2.3 ADSORPTION STUDIES**

Adsorption studies of synthesized  $\text{ZnFe}_2\text{O}_4$  were done in reference to [8]. The concentration of Cr(VI) ions was found out using ICP MS.

## 2.4 CHARACTERIZATION TECHNIQUES

The world of nanoscale materials is a constant bustle of activity as they absorb, emit, break and make bonds. The small size of nanoparticles makes them difficult to catch them<sup>[9]</sup>. There are inherent difficulties in a proper analysis of nanoparticles compared to their bulk counterparts because of their small size and small-scale laboratory production<sup>[10]</sup>. To study these tiny structures, specialized instruments are the only chance.

The invention of a number of high-resolution microscopic techniques in the mid 1980s led to the advancement of nanotechnology to a larger extent. The synthesis methods of nanoparticles through the bottom-up approach where the structures are formed by assembling atoms and molecules got improvised after this<sup>[9]</sup>.

The role of characterization techniques is generally to build a link between the structure, shape, and chemical composition of nanomaterials by processing their diverse properties<sup>[11]</sup>. The increased reactivity at the molecular level is observed in nanoparticles due to their large surface-to-volume ratio. Nanoscale materials show vast diversity in their chemical, electronic, optical, and mechanical properties and by making use of these, extensive studies about them can be made<sup>[10]</sup>.

The important facts to be considered about characterization methods for nanoparticles depend on the type of information which is to be attained by making use of this technique. One or more techniques are employed to acquire the required information of each nanomaterial.

Characterization methods are characterized by analytical and imaging techniques in which the former involves spectroscopy and the latter involves microscopy<sup>[11]</sup>. The primary step of characterization procedures is to reveal crystal structure and chemical composition. The size and shape of the nanoparticles are the other important parameters that are studied through characterization techniques. The size distribution, degree of aggregation, surface charge, surface area, and surface density are the other parameters measured.

The synthesized nanomaterials are subjected to several characterization methods. An evaluation of nanomaterials is done by microscopy, optical microscopy, light scattering, surface scattering, X-ray scattering, Magnetic resonance, Mass spectrometry, and Thermal techniques. The characterization of synthesized nanomaterials is done based on their morphology, surface charge, and size. Several microscopic techniques are employed to study

morphology and it includes Scanning Electron Microscopy (SEM), Field Emission Scanning Electron Microscopy (FE-SEM), Transmission Electron Microscopy (TEM), High-Resolution Transmission Microscopy (HR-TEM), Scanning Tunneling Microscopy (STM), Atomic Force Microscopy (AFM)<sup>[12]</sup>.

### **2.4.1 X-RAY DIFFRACTION**

X-Ray Diffraction is the primary tool for the phase identification of materials. It is a non-destructive technique that gives us information about the lattice structure of a crystalline structure viz unit cell dimensions, bond angles, chemical composition, and the crystallographic structure of the synthesized nanomaterial. This technique is widely used for material identification. The synthesized material is examined by employing this method to check whether it is crystalline or amorphous in nature<sup>[9]</sup>. X-ray diffraction technique is often used for qualitative analysis though it is quantitative in nature and it extends to all crystalline solids viz ceramics, insulators, metals, polymers, organics, powders, thin films, etc. By introducing a variation in the infrastructure, an X-ray diffractometer can be used for a single crystal or powder. The molecular structure can be studied by using a single crystal diffractometer and the analysis of phases is done by using a powder diffractometer, which reveals further molecular information<sup>[13]</sup>.

#### **Theory**

X-rays come in the region between ultraviolet light and gamma rays in the electromagnetic spectrum with the wavelength in the order of 1Å. X-rays are produced by decelerating charged particles using metals which are termed Bremsstrahlung radiation<sup>[13]</sup>.

Electrons that are ejected by thermionic emission from a filament in a vacuum tube are collimated and accelerated by an electric potential of 20-45 KV. This electron beam is then directed towards a metallic anode, which results in electron energy loss and this is manifested as X rays. A small fraction of about 1% of the ejected electron beam gets converted as X rays, whereas the majority energy percentage is dissipated as heat in the metal anode. X-rays produce two kinds of radiation, one is the continuous spectrum comprising a range of wavelengths. This is because the electron that loose energy in a series of collisions with the atoms of the target anode. The nuclear charges in the target anode deflect the radiation emitted by the incident electrons and the continuous spectrum is a result of this<sup>[14]</sup>. The second type is the characteristic spectrum which is produced as a result of a specific electronic transition that takes place within

the individual atoms of the anode. For eg, the characteristic line  $K\alpha$ , X-ray is produced when an electron from the L shell occupies the hole in the K shell and  $K\beta$  is produced when an electron from the M shell occupies the hole in the K shell<sup>[12]</sup>.

A monochromatic beam of a single X-ray wavelength is required and for this, the lines are to be filtered out before undergoing an X-ray spectra study. For this, a crystal monochromator is included in the modern X-ray diffractometer, with a known lattice spacing oriented in such a way that only  $K\beta$  radiation doesn't go unaffected and diffracts only  $K\alpha$  radiation<sup>[12]</sup>. As X rays are electromagnetic rays, they exhibit diffraction and interference. As their wavelengths are in the order of angstroms, ordinary devices like gratings cannot give observable effects. Laue, a German Physicist in 1912 suggested that a crystal consists of a three-dimensional array of regularly spaced atoms that act as grating which differs from the normal grating with the fact that diffracting centers in the crystal are not in one plane, ie., they act more like a space grating than a plane grating. On passing the X-rays, a diffraction pattern will be observed and it will be comprised of a central spot which is as a result of the reflection of some of the incident X-rays from different sets of parallel planes in the crystal which consists of a large number of atoms<sup>[15]</sup>. This is shown in the figure:

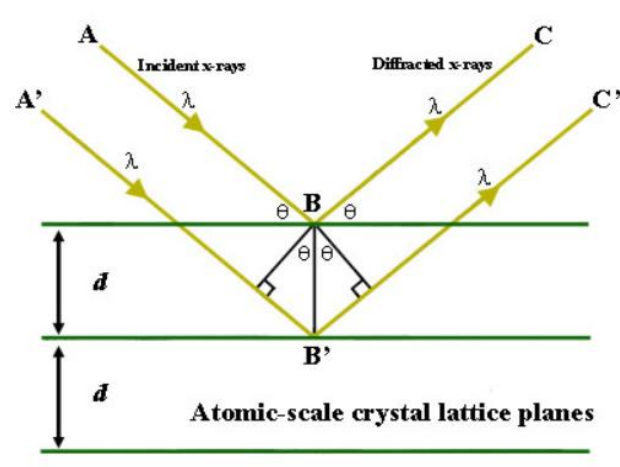


Fig 2.1 (a): Reflection of X Rays from parallel crystal planes<sup>[16]</sup>

### a) Bragg's law for diffraction

W.L. Bragg, formulated Bragg's law for crystalline materials that relates the wavelength of the X rays to the interatomic spacing which is given as:

$$N\lambda = 2d\sin\theta$$

Where,

$\Theta$  is the angle between the diffracted wave and the atomic planes

$\lambda$  is the wavelength of the X-ray beam

$d$  is the interplanar distance

$N$  is the order of the reflection/path difference between waves scattered by adjacent planes of atoms.

Bragg's condition is to be satisfied for the constructive interference to occur i.e., the path difference, which is a whole wavelength ( $\lambda$ ) or its multiple, the two rays continuously interfere and produces a bright spot.

As monochromatic X-rays fall on crystal each atom will act as a site for scattering radiations. In a crystal, there will be few planes that are rich with atoms. The scattered X-rays from these planes are manifested as reflections of these planes. These reflected rays from a set of planes will be in phase with each other, producing maximum intensity. For all angles other than this, the reflections from different planes will be out phase and destructively interfere producing either zero or less intensity<sup>[15]</sup>. Each crystalline material has its own line spectrum. The position and intensity of the line spectrum are used to detect the material. The crystalline phases of the synthesized material can be identified by comparing the XRD data with the fundamental data in Joint Committee on Powder Diffraction Standards (JCPDS)<sup>[9]</sup>.

#### **b) Estimation of crystallite size**

The diffraction peaks are usually broadened and this is due to inhomogeneous strains and this changes from crystals to crystals. This is in proportion with  $\sin\theta$ . The finite size of the crystal is another reason for peak broadening. Here it is independent of  $\sin\theta$ . The crystallite size to peak width can be calculated by the analysis of peak shapes.

The crystallite size  $D$  can be calculated from the peak width using Debye-Scherrer's formula, provided there is no in homogenous strain.

$$D = \frac{K\lambda}{\beta \cos\theta}$$

Where,

$K$  is the Scherrer constant

$\lambda$  is the wavelength of X rays

$\beta$  is the Full-Width Half Maximum (FWHM) of the diffraction peak

$\theta$  is the diffraction angle<sup>[12]</sup>

### **Instrumentation**

The arrangement of an X-ray diffractometer consists of three elements viz X-ray tube, sample holder, and X-ray detector. The monochromatic X-ray beam from the X-ray tube is allowed to fall onto the crystalline material, which is fixed in the sample holder. The diffraction angle  $\theta$  can be varied by rotating the X-ray tube and the detector. A spectrum of diffraction intensity versus the angle between the incident and diffracted beam is recorded by changing the incident angle of the X-Ray beam continuously. The diffracted X-rays are detected by the X-ray detector. A receiving slit is included in the X-ray detector and it is mounted in front of the counter on the counter tube arm and a scatter slit is also included behind it, which ensures that the counter receives radiation only from the region of the sample, illuminated by the incident beam<sup>[16]</sup>. The sample is scanned for arranging of  $2\theta$  angles that give all possible diffraction directions of the lattice. An instrument called the goniometer maintains the angle and rotates the sample<sup>[18]</sup>. Goniometer which serves as the platform holds and moves the sample, optics, detector, sample holder, Receiving-side optics which gives the condition to the X-Ray beam after it has encountered the sample, Detector that counts the number of X-Rays scattered by the sample. For a particular angle  $\theta$ , Bragg's law will be satisfied and the incident radiation produces constructive interferences.



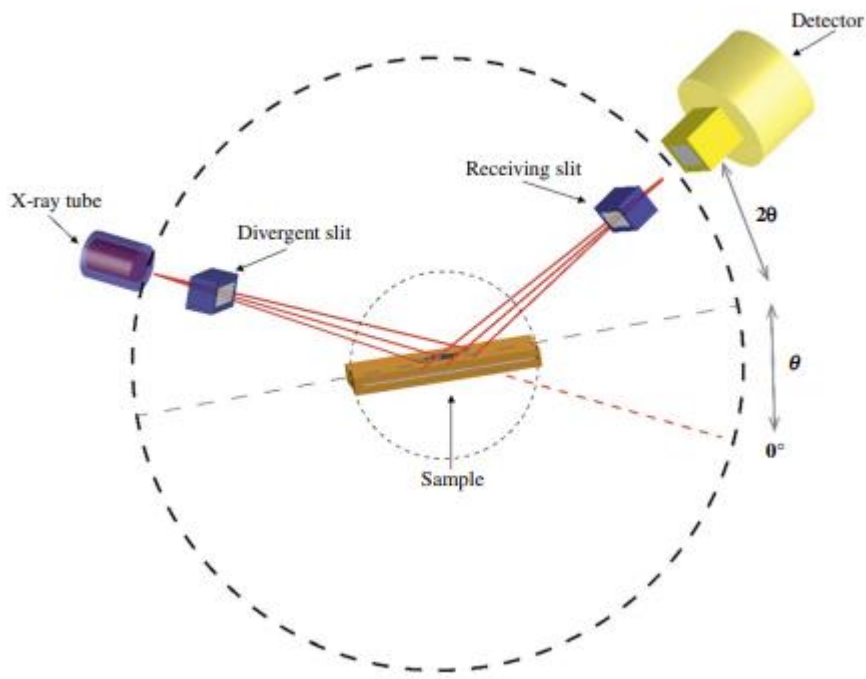


Fig2.1 (b): Basic components of X-Ray Diffractometers<sup>[19]</sup>

The d spacing is unique to every element or compound hence it can be considered the fingerprint of materials. From the XRD data, the d spacing can be found by examining the diffraction peaks and is compared with the standard reference pattern so that the synthesized sample can be identified<sup>[17]</sup>.

## 2.4.2 FOURIER TRANSFORM INFRARED SPECTROSCOPY

Fourier Transform Infrared Spectroscopy is a non-destructive technique that requires no external calibration and gives precise measurements<sup>[20]</sup>. All component frequencies can be varied simultaneously. Infrared spectroscopy is used as an important tool for the identification of the sample and elucidation of its structure. In Infrared spectroscopy, the sample is irradiated with IR radiation. A part of this is absorbed by the sample and the rest of it is transmitted. The resulting spectrum is due to the molecular absorption and transmission and can be attributed to the molecular fingerprint of the sample ie no two distinct and unique molecular structures can produce the same Infrared spectrum<sup>[21]</sup>.

Fourier Transform Infrared Spectroscopy is a characterization technique that is based on the measurement of the absorption of electromagnetic radiation lying within the middle infrared region. All molecules except monoatomic and homopolar diatomic absorb IR radiation whose frequencies affect the dipole moment of the molecule. The dipole moment

arises in a molecule due to the difference of charges in the electronic fields of its atoms. A homopolar diatomic molecule does not possess a dipole moment as its electronic fields are equal. Also, in the case of monoatomic atoms, there is no dipole moment associated with them as they have only one atom. Therefore, they do not absorb IR radiation. Molecules with a dipole moment can only interact with Infrared photons and this paves the way for the molecules to get excited to higher vibrational states. The position of bands that relates to the strength and nature of bands and the presence of functional groups is obtained from the recorded spectrum. Infrared spectroscopy allows the determination of components or groups of atoms that absorb in the Infrared region at specific frequencies from which the molecular structures can be revealed. The constituents in the sample under study vibrate with a frequency that lies in the Infrared region. The oscillations induced by certain vibrational modes provide a means for the matter to couple with radiation and to exchange energy with it when the frequencies are in resonance<sup>[12]</sup>.

## Theory

In Frequency Domain Spectroscopy, the radiant power  $G(\omega)$  is recorded as a function of frequency  $\omega$  whereas, in Time Domain Spectroscopy, the changes in radiant power  $f(t)$  are recorded as a function of time  $t$ . Fourier Transform Infrared Spectroscopy employs this idea where a time domain plot is converted into a frequency domain spectrum. The Fourier transform of the function  $f(t)$  is defined as:<sup>[22]</sup>

$$G(\omega) = \frac{1}{\sqrt{2\pi}} \int_{-\infty}^{+\infty} f(t)e^{i\omega t} dt$$

And the inverse relation:

$$F(x) = \frac{1}{\sqrt{2\pi}} \int_{-\infty}^{+\infty} G(\omega)e^{-i\omega x} d\omega$$

They form the Fourier Transform Pairs.

To explain this, consider the superposition of two sine waves, of the same amplitude with a slight difference in frequencies. The Fourier transform of the individual sine waves and the superimposed wave gives the frequency in the time domain. In this way, complicated time domain spectra could be transformed into frequency domain spectra. High-speed computers are employed for this purpose<sup>[22]</sup>.

## Instrumentation

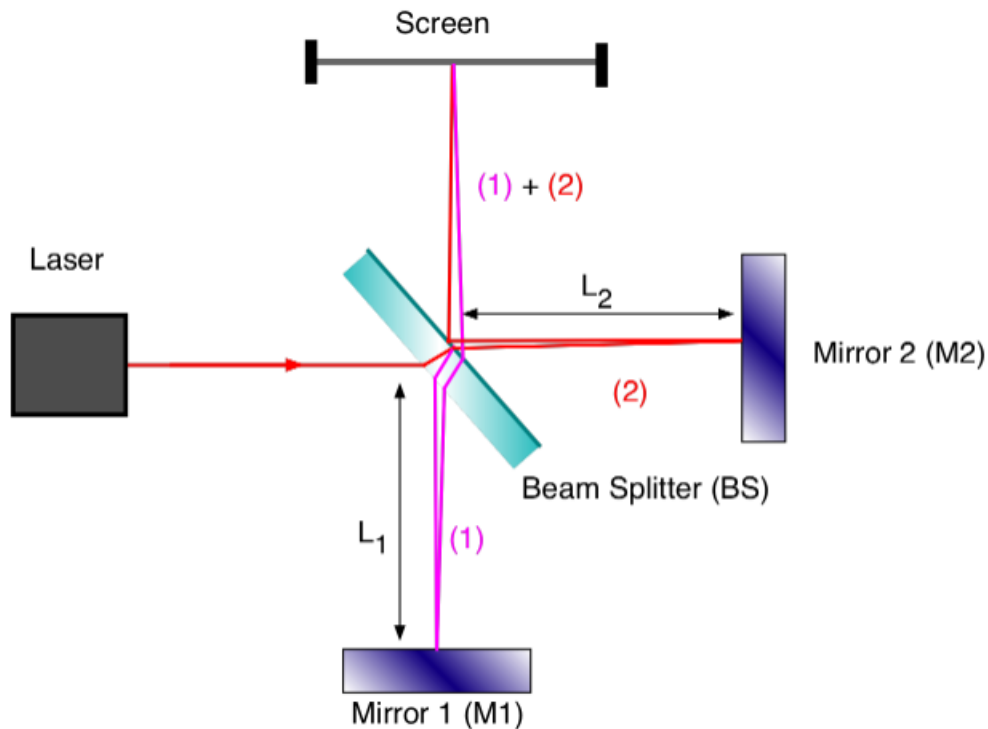


Fig 2.2 (a): Michelson's Interferometer<sup>[20]</sup>

The basic components of Fourier Transform Infrared Spectrometer consist of a source, a beam splitter, plane mirrors, and a detector. The source which is used is the usual glower which is operated at very high temperatures. The Michelson Interferometer consists of a source S, a beam splitter B and two plain mirrors M1 and M2 mounted perpendicular to each other in which the mirror M1 is moveable. The purpose of the beam splitter is to split the beam into two, of equal intensities, and irradiate 50% of the radiation to M1 and the other 50% to M2. The two beams get reflected back to the beam splitter and recombine with 50% going to the source and the other 50% going to the sample. For a monochromatic source, if the path lengths differ by an integral number including zero of wavelengths, constructive interference occurs and if the path lengths differ by a half odd integral number of wavelengths, destructive interference occurs. The mirror M2 is moveable as it is moved towards or away from B, the sample and detector will see an alteration in intensity. If two different monochromatic frequencies are used, a more complicated interference pattern would follow as M2 is moved. The two originals with appropriate intensities are obtained from the Fourier Transform of the resultant signal. As an extension of this, when white light is employed, an extremely complicated interference pattern is transformed back to the original frequency distribution. As

the recombined beam is directed through a sample, the sample absorption will be shown as gaps in the frequency distribution whose transformation gives a normal absorption spectrum. The signal from the detector is fed to a multichannel computer as mirror M2 is moved. The computer does the Fourier Transform of the stored data and it is plotted<sup>[22]</sup>.

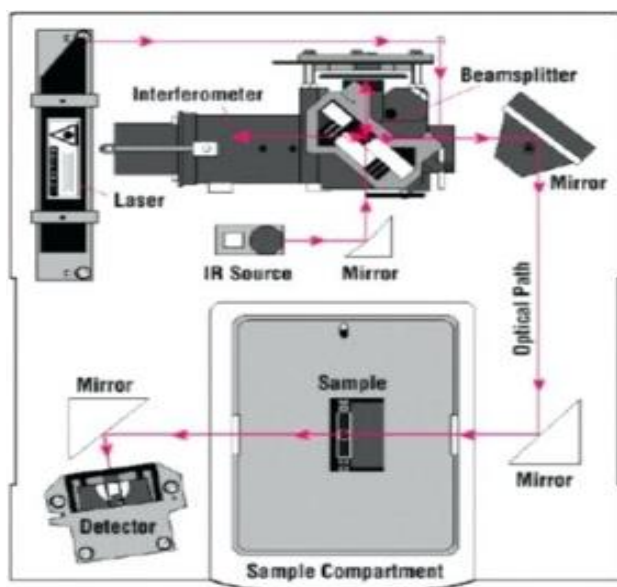


Fig 2.2(b): Schematic diagram of FTIR<sup>[20]</sup>

### Preparation of the sample for FTIR

For a solid sample, the sample powder is ground with KBr and this is made into a pellet and introduced onto the FTIR instrument. KBr is used as a carrier for the sample as it is optically transparent for the light in the IR range. KBr has a 100% transmittance in the (4000-400) $\text{cm}^{-1}$  range of wavenumber. The sample under study clearly will not have this 100% transmittance and this helps us to take the absorption behavior of our sample under study.

### 2.4.3 SCANNING ELECTRON MICROSCOPY

Scanning Electron Microscopy is one of the resourceful techniques which is used for studying microstructure morphology and for chemical composition characterizations. The discovery of the new principle that the electrons get deflected in the presence of a magnetic field outscored light microscopy. The replacement of high-energy electrons over the light source has brought a new dawn to scientific research through electron microscopy<sup>[23]</sup>. The surface topography, crystalline structure, chemical composition, and electrical behavior of the material can be analyzed by the SEM technique. Despite the surface roughness, SEM ensures a large depth focus on the specimen<sup>[24]</sup>. The resolution of the SEM ranges in nanometers and

the magnification can go in the range from 10 to 300,000. The chemical composition at the surface of the sample can be known from the scanning electron micrographs in addition to topological information <sup>[9]</sup>. The specimen whose micrographs are to be taken is attached to a sample holder called the “Stub” and a very short preparation time is needed. Therefore, a nondestructive evaluation of the specimen is assured by SEM<sup>[24]</sup>.

## **Theory**

### **1) Electron-Sample Interaction**

An image is formed from SEM by obtaining the signals that arise from the electron beam-specimen interaction. The interactions can be either elastic or inelastic. The specimen nucleus or outer shell electrons with similar energy to that of the incident electrons deflect them which attributes to a negligible energy loss during the collision and there is a wide-angle directional change of the scattered electron resulting in elastic scattering. Backscattered electrons are the electrons that underwent elastic scattering through an obtuse angle and are widely used for imaging the sample. Various interactions that take place between specimen atoms and the incident electrons result in a primary electron beam that transfers substantial energy to the atom and this attributes to the inelastic scattering. The amount of energy loss matters as to whether the excitation of electrons was done singly or collectively and also on the binding energy of the electron to the atom. The secondary electrons arise from the excitation of the specimen electrons by the ionization of the specimen atoms and they possess energies less than 50eV which is also used for imaging and analyzing the sample. Characteristic X-rays, Auger electrons, and cathodoluminescence are the other means by which the imaging is done by the resulting signals<sup>[23]</sup>.

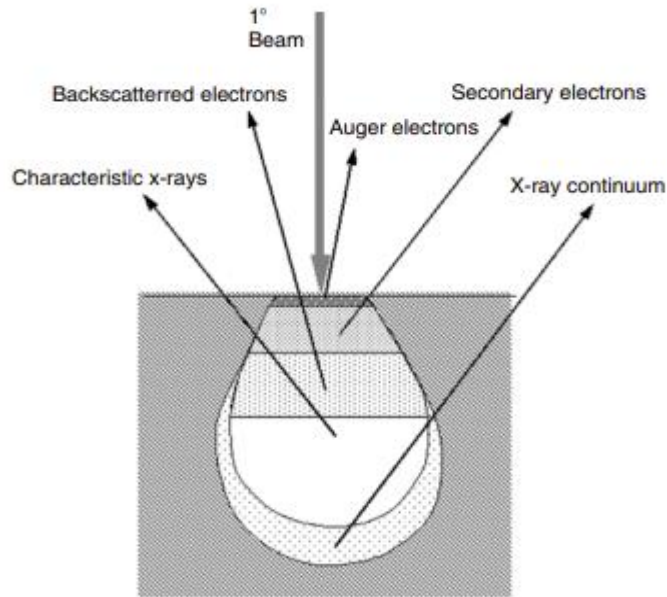


Fig 2.3 (a): Signals generated by the interaction of specimen-electron beam in the Scanning Electron Microscope<sup>[23]</sup>.

Whenever the incident electron beam strikes the specimen surface, most of the time the energetic electrons penetrate onto the sample for some distance instead of just bouncing off before they collide with the specimen atom. This results in the formation of the primary electron beam. This is called the region of excitation where several signals are produced. The electron beam energy and the electron density influence the size and shape of this region. When the accelerating voltage reaches a certain point, for a low atomic number specimen the shape of the interaction volume will be teardrop, and for a specimen with a higher atomic number, the shape of the interaction volume will be a hemisphere. The depth and volume of the penetration are directly proportional to the beam energy and inversely related to the atomic number. This is because as the number of electrons is high they act as a barrier to the penetration. On applying high accelerating voltage, the penetration length will be deep resulting in a large primary excitation region which results in the loss of surface resolution and the surface of the spheres will look smooth<sup>[23]</sup>.

**i) Secondary Electrons**

They are the most widely used signal for imaging. Secondary electrons are produced when the primary electron beam strikes the sample surface and ionizes the atoms of the specimen. This causes the loosely bound electrons to get emitted called the secondary electrons. Due to its low energy in the range of 3-5 eV, they can only escape only a few

nanometers distance from the proximity of the sample surface. This aids us to get the topographic information of the sample with a good resolution. Therefore, an image produced in such a manner will depend on the number of secondary electrons that reach the detector. The secondary electrons whose way towards the detector is when obstructed result in casting shadows resulting in a darker region compared to other regions that had unobstructed electron path to the detector. Therefore, we can say that the imaging also depends on the position of the detector<sup>[23]</sup>.

**ii) Backscattered electrons**

The topological and compositional information of the sample is revealed from the signal generated from the backscattered electrons. A backscattered electron will have an energy greater than 50 eV that escapes from the sample surface after undergoing a single or multiple scattering event. The backscattering signal is higher for elements with higher atomic numbers, i.e., the backscattered yield is proportional to the atomic number. BSE gives the deep surface information<sup>[23]</sup>.

**iii) Characteristic X rays**

The interaction of the sample with the primary electron beam results in characteristic X rays and its analysis is used to understand the chemical information which is widely used in the microanalytical technique in SEM. When the primary electron ejects out an electron from the inner shell an electron from the outer shell replaces the inner shell electron resulting in the release of an X-ray photon, bringing the ionized atom back to the ground state. The *Bremsstrahlung* radiation will constitute a background noise and this is usually removed from the spectrum before analysis though it contains the information for quantification of the emitted spectrum<sup>[23]</sup>.

**iv) Auger Electrons**

The excess energy released when an electron from the outer shell recombines with the inner shell hole of an ionized atom is carried by an Auger electron. Auger electrons are emitted near the surface due to low energy and are therefore used for surface analysis<sup>[23]</sup>.

**v) Cathodoluminescence**

When the specimen undergoes collision with the primary electron beam and the vacancy thus created is filled by electrons and the resulting excess energy is released as infrared/Ultraviolet/visible range photons. These photons are detected and used for energy stabilization. They have an image resolution of about 50nm<sup>[23]</sup>.

**vi) Transmitted Electrons**

Transmission electrons are made used to obtain images of the ultrathin specimen where the primary beam electrons can pass through it. Thus this method allows us to understand the ultrastructure of thin specimens. The elemental information and distribution can be understood by integrating the transmitted electrons with X-ray microanalysis<sup>[23]</sup>.

**vii) Specimen current**

The difference between the primary electron beam and the sum of the backscattered, secondary, and Auger electrons is defined as the Specimen current. The emission current that a specimen has is inversely proportional to the specimen current. In this technique, the sample is itself its detector<sup>[23]</sup>.

**ii) Specimen Preparation**

Most of the nanomaterials including carbon nanotubes, nanowires can be directly observed just by loading on carbon tape, and therefore the sample preparation is so simple whereas, in the case of nonconducting materials such as bio-organic nanomaterials, a metal coating is to be given which makes the sample preparation much difficult<sup>[23]</sup>.

**Instrumentation**

A conventional SEM has a column structure that consists of an electron gun on top of the column, Electromagnetic lenses, apertures for collimating the beam onto the specimen, a high vacuum environment for the electron to travel with no scattering with the air, a processing system to obtain real-time observation and image recording of the specimen surface<sup>[23]</sup>.



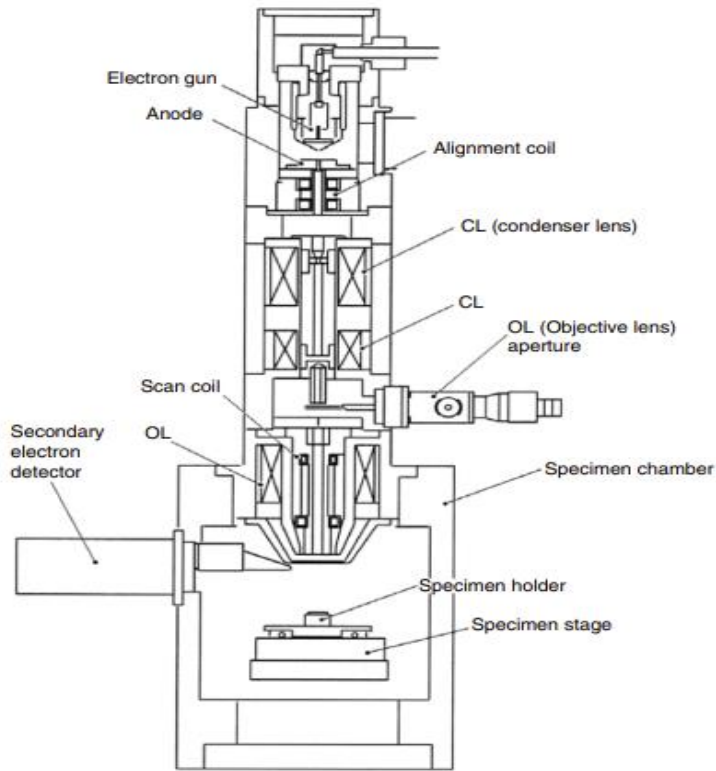


Fig 2.3 (b): Schematic of SEM <sup>[23]</sup>.

## 1) Electron Guns

The electron gun produces an electron beam with a high current that is stable, small spot size, adjustable energy, and small energy dispersion are the requirements of an SEM system. Various types of electron guns are employed in an SEM and the electron beams that are produced by them differ in their quality. Electron guns are chosen by giving importance to emitter lifetime. Field emission guns are used in the modern SEM system which is of 3 types, Cold Field Emission source in which the electron source act at room temperature, the thermal Field Emission source which is operated at higher temperatures, and the Schottky emitters<sup>[23]</sup>.

## 2) Electron Lenses

Electron beams are controlled by a magnetic field which ensures a small deviation. Electromagnets which are made by coiling the wire are used for magnetic fields and a current is applied to these coils which control the path of the electrons. As its strength can be varied they are capable of magnifying and de-magnifying the beam diameter by which the focal length can be adjusted. SEM needs a narrow beam to scan the surface of the specimen<sup>[23]</sup>.

### i) Condenser lenses

Condenser lenses are mainly two rotationally symmetric iron pole pieces with a copper winding that produces magnetic fields. The electron beam passes through the hole given

at the centre of the pole pieces. The electron beam that diverges after passing through the anode plate from the emission source is converged and collimated by this setup. The two pole pieces are separated by a lens gap where the focusing of the electron beam is done by the magnetic field. The condenser lens current is tuned to adjust the focal point. A condenser aperture with an appropriate aperture size is chosen to expel inhomogeneous and scattered electrons. By including a second condenser lens, additional control over the electron can be achieved<sup>[23]</sup>.

### **ii) Objective lenses**

Further demagnification is given to the electron beam that diverges below the converging aperture and is focused on a probe point at the specimen surface. The image resolution is enhanced by reducing the electron diameter by choosing the appropriate lens and its aperture size<sup>[23]</sup>.

## **3) Column Parameters**

The image quality is influenced by various parameters viz, aperture, working distance, electron beam energy, lens current, chromatic, and achromatic aberration of electron lenses<sup>[23]</sup>

### **i) Aperture**

Apertures are used to lessen the spherical aberrations of the final lens and also to eliminate the scattered electrons. In an SEM system, two types of apertures are seen viz real aperture which is at the base of the final lens, and the virtual aperture which is placed a point above the final lens. The real aperture shapes the beam and adjusts its edge whereas the virtual aperture limits the electron beam<sup>[23]</sup>.

### **ii) Stigmation**

The shape of the cross-section electron beam profile changes shape due to the defects in the lens, and contamination in the aperture or column. So an elliptical cross-section instead of a circular one is formed and this imperfection in the electromagnetic lens is called astigmatism which results in the stretching of the image in different directions at over focus and under focus conditions. To overcome this, a series of coils are given surrounding the electron beam called the stigmator to obtain a high-resolution image<sup>[23]</sup>.

### **iii) Depth of the field**

Depth of the field is defined as the portion of the image that comes under the focus and this is dependent on how small the convergence angle of the electron beam is. When it comes to observing a specimen with wide topological variation, depth of field matters<sup>[23]</sup>.

#### 4) Image formation

As an electron beam falls on the surface of the specimen, a number of complex interactions take place as a result of which a number of signals are produced. All the types of electrons are collected and analyzed to decode the information regarding the specimen<sup>[23]</sup>.

##### i) Secondary Electron detectors

As secondary electrons are of low energy, they are capable of giving information about giving information regarding the surface topography and chemistry. The collection of such low-energy electrons will result in noise and using an electron multiplier is a solution. So these electrons are directed toward the cathode and secondary electrons are produced. These electrons are then directed to a secondary cathode for further signal multiplication. This process is repeated several times, and amplified in such a way that the image can be processed<sup>[23]</sup>.

##### ii) Specimen magnification

Magnification is defined as the ratio of the scanning length of the cathode ray tube image to its scanning line on the specimen<sup>[23]</sup>.

#### 5) Vacuum System

The scattering on the electron beam and the contamination of the electron guns is avoided by an ultrahigh vacuum system therefore it's an inevitable part of SEM. Several types of pumps are employed to get the desired vacuum environment. The mechanical pumps and a diffusion pump bring down the chamber from atmospheric pressure<sup>[23]</sup>.

### 2.4.4 INDUCTIVELY COUPLED PLASMA MASS SPECTROMETRY

Inductively Coupled Plasma Mass Spectrometry (ICPMS) is a highly sensitive mass spectroscopic technique that can determine at a concentration of below one part of 1ppm of several elements including metals and nonmetals. This analytical technique is used for the separation of ions and elemental determination. This method offers high speed, precision, and sensitivity than what is seen in Atomic Absorption Spectrometer<sup>[25]</sup>.

The plasma source in which the energy is given by the electric currents generated by electromagnetic induction is termed the Inductive Coupled Plasma (ICP) which has two geometries viz planar and cylindrical. The electrode will have a spiral shape for planar ICP and will be helical for cylindrical ICP. ICPMS is widely used in several fields such as wastewater treatment, hydrogeology, soil science, metallurgy, mining, and food sciences<sup>[25]</sup>.

## Detection Limit

This is shown in the following table: <sup>[25]</sup>.

Element	Detection limit (ppt)
U, Cs, Bi	Less than 10
Ag, Be, Cd, Rb, Sn, Sb, Au	10-50
Ba, Pb, Se, Sr, Co, W, Mo, Mg	50-100
Cr, Cu, Mn	100-200
Zn, As, Ti	400-500
Li, P	1-3 ppb
Ca	less than 20 ppb

Table 1 (a): Detection limit of various elements

## Elemental Analysis

Elements with atomic mass in the range of 7-250 can be analyzed using ICPMS. Atomic masses viz 40, 56, and 80 are excluded because of too much content of Argon<sup>[25]</sup>.

## Principle of Operation

ICPMS are of several designs. The chief components of an ICPMS instrument are a nebulizer, spray chamber, plasma torch, interface, mass spectrometer, detector, and mass separation device. The sample in its liquid form is pumped into a nebulizer which converts it into its aerosol form along with the argon gas. About 1-2% of this form enters the spray chamber. The spray injector pushes this fine aerosol onto the plasma torch. The plasma torch ionizes the gas with the aid of an intense magnetic field. The photons are prohibited from reaching the detector to prevent signal noise. The ions produced in the plasma enter the interface region which is kept in a vacuum state from which they are directed to the mass spectrometer. The interface region guides the ion towards the mass separation device<sup>[25]</sup>.

The interface consists of a sampler and a skimmer that are two metallic cones. The role of the interface region is very crucial in that it has to guide the ions from a region of atmospheric pressure to a region of a vacuum of  $10^{-8}$  torr. A potential difference of hundred volts is produced due to the capacitive coupling of the RF coil and the plasma. This is avoided as this would result in an electric discharge between the plasma and the sampler cone which aids in the formation of interfering species that makes the optimization of ion optics unpredictable by influencing the kinetic energy of the ion species that enter the mass spectrometer. This is done by placing a grounding strap between the coil and the interface

region, including a shield that is grounded between the coil and the plasma torch, and by using a double interlaced coil<sup>[25]</sup>.

A series of electromagnetic lenses called ion optics directs the ions extracted from the interface region to the main vacuum chamber where the vacuum is maintained by a turbo molecular pump. The mass separation device allows the analyte ions of a particular mass to charge ratio to enter the detector such that the rest of the non-analyte, interfering, and matrix ions get eliminated. This can either be a scanning or a simultaneous process depending upon the design of the mass spectrometer. The ions are then converted to an electric signal by the ion detector which is usually a dynode detector that mainly comprises a series of dynodes along the length of the detector. When the ions touch a dynode they are converted to electrons and these electrons get attracted to the next dynode, this happens till the last dynode and there will be a high electron stream after this. The data handling system process this data and converts it into analyte concentration as per the ICPMS calibration standards<sup>[25]</sup>.

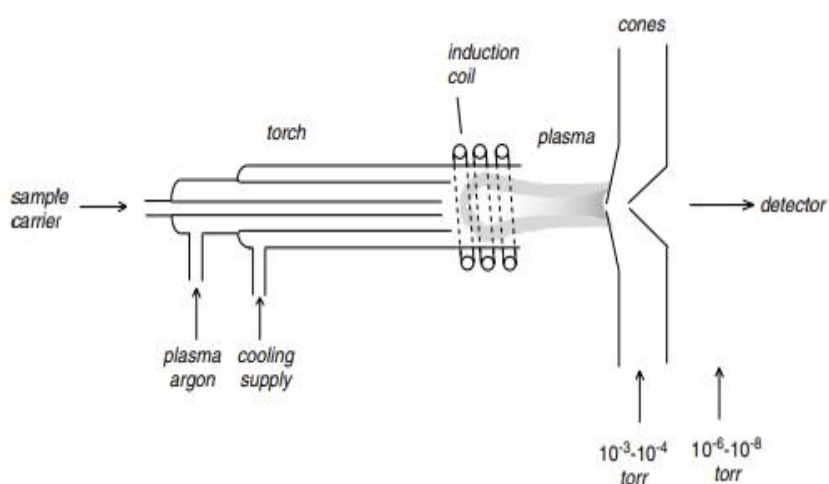


Fig2.4 (a): Ion source and interface in ICP MS<sup>[26]</sup>.

## Sample Preparation

The International Standard is the chief component which also acts as the diluent. It consists of Nitric/hydrochloric acid along with deionized water along with Indium or Gallium. 5mL of this and 10-500microlitres of the sample are taken and vortexed for several times and then loaded into the autosampler tray. The viscous sample is to be digested before analysis<sup>[25]</sup>.

## Instrumentation

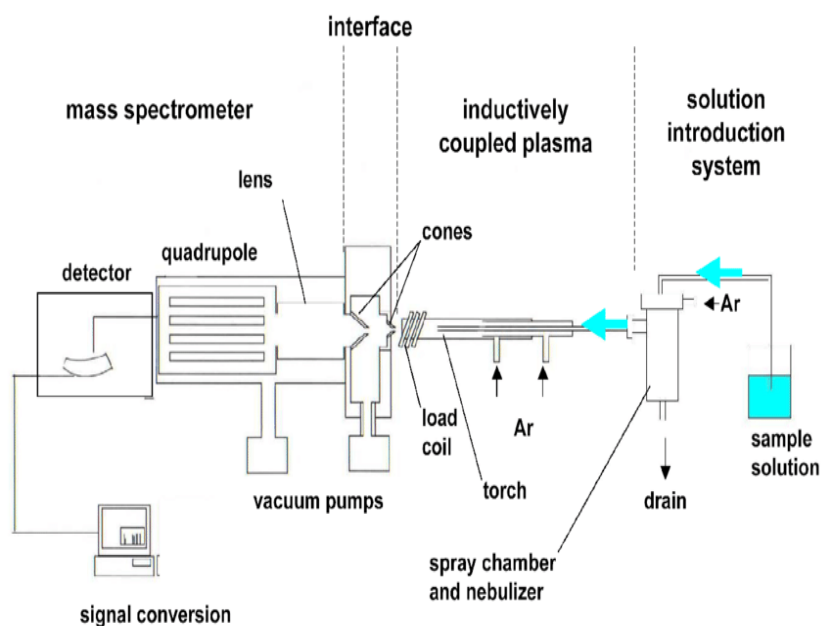


Fig 2.4 (b): Schematic diagram of ICP MS<sup>[27]</sup>.

### i) Sample Introduction

The sample is introduced as a part of the first step in the procedure. Solids and liquid samples are acceptable for the ICPMS analysis. The liquid samples are introduced onto a nebulizer which converts them into an aerosol which is then allowed to enter a spray chamber where a drain removes the larger droplets. Solid samples are introduced via a laser ablation system where the sample is exposed to a laser and it creates a crest of the ablated sample and this can be swept into plasma<sup>[25]</sup>.

### ii) Sample Ionization

After the desolvation of the sample in the nebulizer, it gets mixed with more argon gas as it enters the torch body. A coil setup is given to produce an argon plasma by transmitting radio frequency to the heated argon gas. Any solvent that remains if any is removed by this argon plasma<sup>[25]</sup>.

### iii) ICPMS Interface

The interface that exists between the Inductively Coupled Plasma and the Mass Spectrometer has a major role in creating a vacuum for the Mass Spectrometer region. The ionization occurs at atmospheric pressure and by creating a vacuum space, ions are allowed to move freely without any collision with air molecules<sup>[25]</sup>.

#### iv) Plasma Torch

A partially ionizing gas Argon is used for creating plasma and the sufficient energy for this is given by the electric current from the wires around the Argon gas. The plasma torch consists of three concentric tubes which are made of quartz. There is an induction coil supplied with a radio frequency (RF) current into which the end of the torch is placed. An electric spark is given to the argon air that passes between two tubes and this results in the release of electrons onto the gas stream which is then influenced by the RF magnetic field and gets accelerated<sup>[25]</sup>.

#### v) Mass Spectrometer

A pump extraction system which is included in the first stage of the Mass Spectrometer expels the ions from the plasma. The ion beam produced is focused on another unit. The isotopes are removed as per their charge to the mass ratio by employing various types of mass analyzers. An example of such an analyzer is the quadrupole analyzer which is compact but for ions with the same mass to charge ratio it gives a low resolution. A quadrupole filter is to use and it consists of four metal rods that are aligned parallelly, in a diamond pattern. An electrical potential of combined AC and DC is applied to the rods of opposite potentials. A single ion with a specific mass to charge ratio will be allowed a path by setting a single value of AC and DC. A combination of these potentials allows an array of ions with different  $m/z$  ratios for detection<sup>[25]</sup>.

#### vi) Detector

A channeltron multiplier is often used as the detector in ICPMS. It is a corn-shaped tube with high voltage supplied and has an opposite charge to the ions which is to be detected. This enables the interior cone to attract and collect the ions that leave the quadrupole filter. Secondary electrons are emitted when they strike the surface. This process repeats<sup>[25]</sup>.

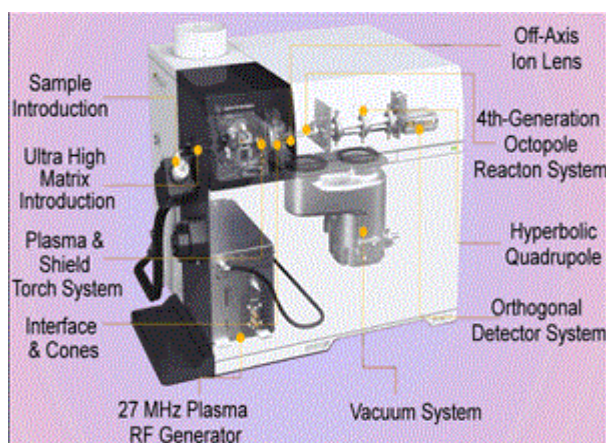


Fig 2.4 (c): ICP MS Instrument<sup>[28]</sup>

## REFERENCES

1. Singh, N. B., and Anupam Agarwal. "Preparation, characterization, properties and applications of nano zinc ferrite." *Materials Today: Proceedings* 5.3 (2018): 9148-9155.
2. Shahraki, R. Raeisi, et al. "Structural characterization and magnetic properties of superparamagnetic zinc ferrite nanoparticles synthesized by the coprecipitation method." *Journal of Magnetism and Magnetic Materials* 324.22 (2012): 3762-3765.
3. Houshiar, Mahboubeh, et al. "Synthesis of cobalt ferrite (CoFe<sub>2</sub>O<sub>4</sub>) nanoparticles using combustion, coprecipitation, and precipitation methods: A comparison study of size, structural, and magnetic properties." *Journal of Magnetism and Magnetic Materials* 371 (2014): 43-48.
4. Bader, N. A. B. I. L., ABDULSALAM A. Benkhayal, and B. Zimmermann. "Co-precipitation as a sample preparation technique for trace element analysis: an overview." *Int. J. Chem. Sci* 12.2 (2014): 519-525.
5. Kurian, Manju, and Divya S. Nair. "Effect of preparation conditions on nickel zinc ferrite nanoparticles: a comparison between sol-gel auto combustion and coprecipitation methods." *Journal of Saudi Chemical Society* 20 (2016): S517-S522.
6. Romao, C. P., et al. "Negative thermal expansion (thermomimetic) materials." (2013): 127-151.
7. Arulmurugan, R., et al. "Effect of zinc substitution on Co-Zn and Mn-Zn ferrite nanoparticles prepared by co-precipitation." *Journal of Magnetism and Magnetic Materials* 288 (2005): 470-477.
8. Nizam, Thanooja, et al. "Adsorption efficiency of sol-gel derived nano metal ferrites, MFe<sub>2</sub>O<sub>4</sub> (M= Ni, Zn, Cu) on the removal of Cr (VI) ions from aqueous solution." *Journal of Sol-Gel Science and Technology* 101.3 (2022): 618-629.
9. Thomas Varghese, K. M. Balakrishna: "Nanotechnology: An Introduction to Synthesis, Properties, and Applications of Nanomaterials, Atlantic Publishers & Distributors (P) Ltd
10. Mourdikoudis, Stefanos, Roger M. Pallares, and Nguyen TK Thanh. "Characterization techniques for nanoparticles: comparison and complementarity upon studying nanoparticle properties." *Nanoscale* 10.27 (2018): 12871-12934.
11. Daniel L. Schodek, Paulo Ferreira: "Nanomaterials, Nanotechnologies and Design", © 2009, Elsevier Ltd.



12. Salame, Paresh H., Vijay B. Pawade, and Bharat A. Bhanvase. "Characterization tools and techniques for nanomaterials." *Nanomaterials for green energy*. Elsevier, 2018. 83-111.
13. T.Pradeep, Nano: The Essentials, Understanding Nano Science and Nanotechnology, Tata McGraw-Hill Publishing Company Limited, NEW DELHI
14. M. A. Wahab: "Solid State Physics: Structure and properties of materials", Narosa Publishing House, 1999-Science
15. S. O. Pillai: Solid State Physics Structure and Electron properties, Wiley Eastern Limited New Age International Limited
16. [https://serc.carleton.edu/research\\_education/geochemsheets/BraggsLaw.html](https://serc.carleton.edu/research_education/geochemsheets/BraggsLaw.html)
17. "Basic Principle, Working and Instrumentation of Experimental Techniques" Chapter 2, Ph. D. Thesis" Nikita H. Patel
18. Bunaciu, Andrei A., Elena Gabriela Udriștioiu, and Hassan Y. Aboul-Enein. "X-ray diffraction: instrumentation and applications." *Critical reviews in analytical chemistry* 45.4 (2015): 289-299.
19. Falsafi, Seid Reza, Hadis Rostamabadi, and Seid Mahdi Jafari. "X-ray diffraction (XRD) of nanoencapsulated food ingredients." *Characterization of nanoencapsulated food ingredients*. Academic Press, 2020. 271-293.
20. [https://www.niu.edu/analyticallab/\\_pdf/ftir/FTIRintro.pdf](https://www.niu.edu/analyticallab/_pdf/ftir/FTIRintro.pdf)
21. Park, Hae-Sung, et al. "Evaluating Interfacial Adhesion Properties of Pt/Ti Thin-Film by Using Acousto-Optic Technique." *Journal of the Korean Society for Nondestructive Testing* 36.3 (2016): 188-194.
22. G. Aruldas, Molecular Structure, And Spectroscopy, Prentice-Hall Of India-2007
23. Zhou, Weilie, et al. "Fundamentals of scanning electron microscopy (SEM)." *Scanning microscopy for nanotechnology*. Springer, New York, NY, 2006. 1-40.
24. Vernon-Parry, K. D. "Scanning electron microscopy: an introduction." *III-Vs Review* 13.4 (2000): 40-44.
25. <http://www.ijrpc.com/files/14-2111.pdf>
26. Ammann, Adrian A. "Inductively coupled plasma mass spectrometry (ICP MS): a versatile tool." *Journal of mass spectrometry* 42.4 (2007): 419-427.
27. Gilstrap Jr, Richard Allen. *A colloidal nanoparticle form of indium tin oxide: system development and characterization*. Georgia Institute of Technology, 2009.
28. <https://crf.iitd.ac.in/fecility-icp-ms.html>

# CHAPTER 3

## RESULTS AND DISCUSSIONS

Zinc Ferrite ( $\text{ZnFe}_2\text{O}_4$ ) nanoparticles were synthesized by adopting a bio approach with plant extract mediated procedure. *Zingiber officinale* was used as the stabilizing agent. The synthesized sample was structurally and optically characterized using X-Ray Diffraction, and Fourier Transform Infrared Spectroscopy respectively. The morphology of the sample was examined by Scanning Electron Microscopy. Batch adsorption studies were performed and the percentage removal of Cr (VI) was calculated from the results of Inductively Coupled Plasma Mass Spectroscopy. The details of the results of characterizations are discussed as follows.

### 3.1 PHASE IDENTIFICATION: X-RAY DIFFRACTION (XRD)

The crystal structure, as well as the purity of the synthesized ferrite sample, was studied by recording the X-ray diffraction pattern (X'pert3 Powder model). XRD pattern of as-synthesized  $\text{ZnFe}_2\text{O}_4$  was recorded. Fig 3.1(a) represents the X-ray diffraction patterns of  $\text{ZnFe}_2\text{O}_4$  samples calcined at different temperatures. In the figure, C0 represents a sample without calcination. C1, C2, C3, and C4 represent samples calcined at 100°C, 200°C, 300°C, and 400°C for 1 hour respectively.

From the figure, it is evident that C0 and C1 shows broad XRD patterns indicate their amorphous nature. The sample becomes crystalline from calcination temperature 200°C (C2) and the complete phase formation is was identified at 400°C (C4).

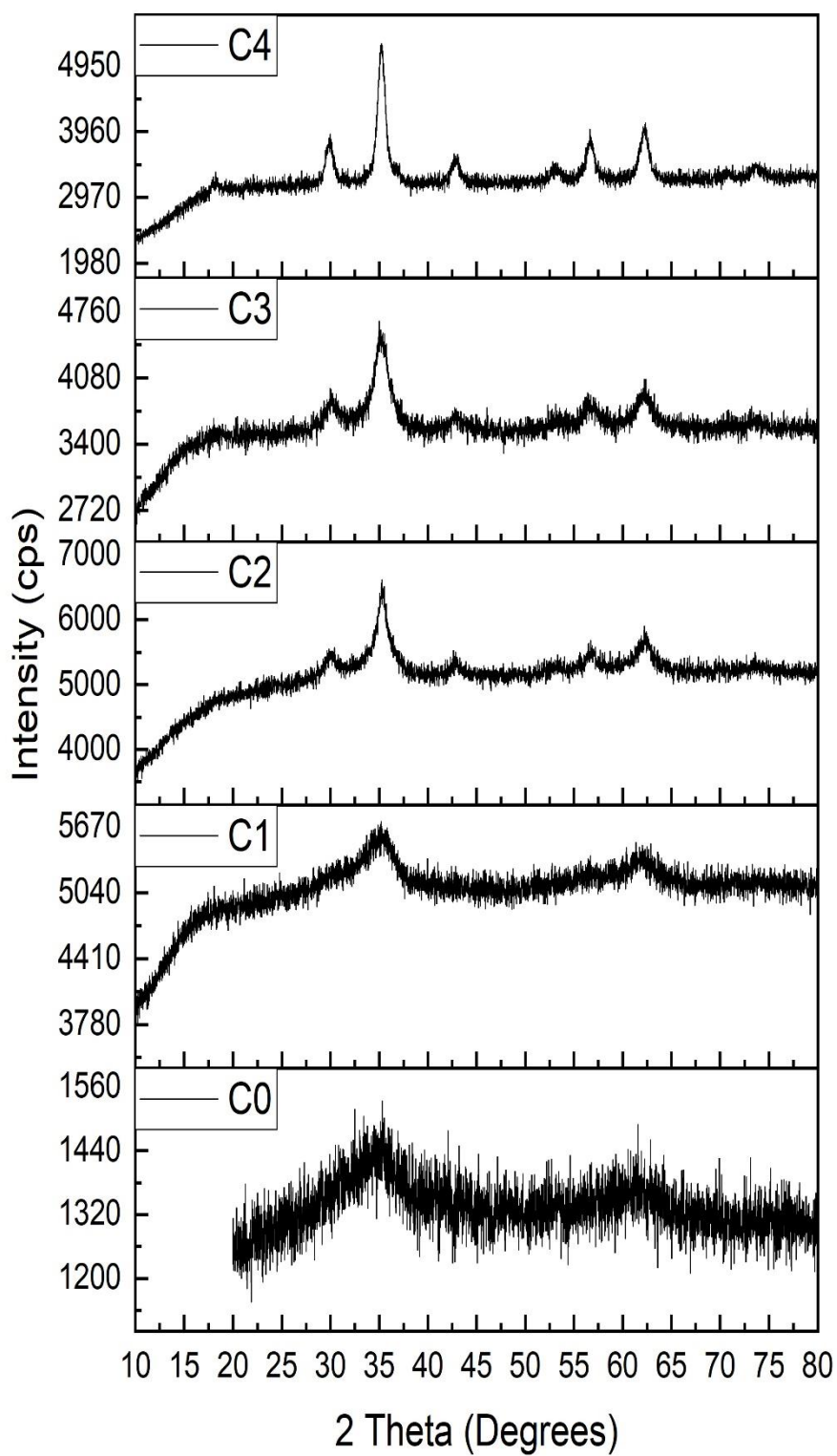


Fig 3.1 (a): X-Ray Diffraction pattern of ZnFe<sub>2</sub>O<sub>4</sub> nanoparticles calcined at different temperatures

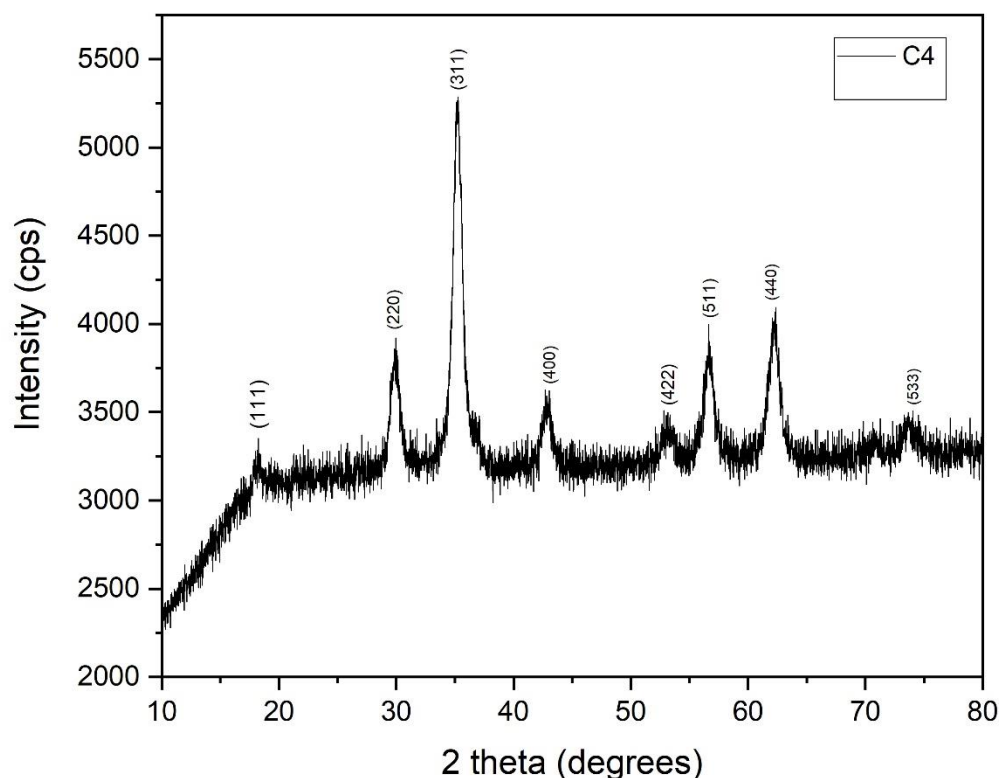


Fig 3.1 (b): X-Ray diffraction pattern of  $\text{ZnFe}_2\text{O}_4$  nanoparticles calcined at  $400^\circ\text{C}$  (C4)

The XRD pattern of the sample was compared and indexed with standard JCPDS data (JCPDS entry: 01-089-1011). Fig 3.1(b) shows the XRD pattern of  $\text{ZnFe}_2\text{O}_4$  calcined at  $400^\circ\text{C}$  (C4). The characteristic peaks of the sample is observed at  $2\theta = 35.27^\circ$ ,  $62.17^\circ$ ,  $56.65^\circ$ ,  $29.89^\circ$ ,  $42.88^\circ$ ,  $53.12^\circ$ ,  $73.84^\circ$ , and  $18.21^\circ$  representing their respective crystal planes (311), (440), (511), (220), (400), (422), (533), and (111). The sharpness of XRD peaks indicates the good crystalline nature of the synthesized nanoparticles which could enable the adsorptive properties of the sample. No traces of any impure phases are obtained which confirms the formation of  $\text{ZnFe}_2\text{O}_4$  of single-phase cubic symmetry with spinel structure

### 3.1.1 Estimation of average crystallite size

The average crystalline size of the samples was calculated from the XRD pattern using the Debye-Scherrer formula:

$$D = \frac{K\lambda}{\beta \cos\theta}$$

Where K is the Scherrer constant.

$\lambda$  is X-Ray Ray wavelength (Cu K $\alpha$  radiation with a wavelength of 0.154 nm)

$\theta$  is the Bragg Diffraction Angle

$\beta$  is the Full-Width Half Maximum (FWHM) of the XRD peak appearing at the diffraction angle  $\theta$ .

This was done by two methods,

**i) Single peak fitting**

For the calculations FWHM of the maximum intensity peak observed at 35.27°, (311) plane was used. The crystallite size was calculated using the Debye Scherrer equation.

$$D = \frac{K\lambda}{\beta \cos\theta}$$

Here, K = 0.89

$$\lambda = 0.154 \text{ nm}$$

$$2\theta = 35.23$$

$$\beta = 1.023$$

$$D = \frac{0.89 \times 0.154}{1.023 \times \frac{\pi}{180} \cos\left(\frac{2 \times 35.23}{2} \times \frac{\pi}{180}\right)} = \underline{7.67 \text{ nm}}$$

**ii) Multiple peak fitting**

For the calculations, FWHM of peaks observed at  $2\theta = 35.27^\circ, 62.17^\circ, 56.65^\circ, 29.89^\circ$  with (311), (440), (511), (220) planes respectively were used. The crystallite size was calculated using the Debye Scherrer equation.

$$K = 0.89$$

$$\lambda = 0.154 \text{ nm}$$

1)  $2\theta = 35.23$

$$\beta = 1.057$$

$$D = \frac{0.89 \times 0.154}{1.057 \times \frac{\pi}{180} \cos\left(\frac{2 \times 35.23}{2} \times \frac{\pi}{180}\right)} = \underline{7.42 \text{ nm}}$$

$$2) \quad 2\theta = 62.21$$

$$\beta = 1.391$$

$$D = \frac{0.89 \times 0.154}{1.391 \times \frac{\pi}{180} \cos\left(\frac{2 \times 62.21}{2} \times \frac{\pi}{180}\right)} = \underline{5.64 \text{ nm}}$$

$$3) \quad 2\theta = 56.64$$

$$\beta = 1.435$$

$$D = \frac{0.89 \times 0.154}{1.435 \times \frac{\pi}{180} \cos\left(\frac{2 \times 56.64}{2} \times \frac{\pi}{180}\right)} = \underline{5.47 \text{ nm}}$$

$$4) \quad 2\theta = 29.91$$

$$\beta = 0.997$$

$$D = \frac{0.89 \times 0.154}{0.997 \times \frac{\pi}{180} \cos\left(\frac{2 \times 29.91}{2} \times \frac{\pi}{180}\right)} = \underline{7.87 \text{ nm}}$$

The average of these four values are is given by:

$$\frac{7.42 + 5.64 + 5.47 + 7.87}{4} = \underline{6.6 \text{ nm}}$$

The average crystallite size of the sample found was about 7.67nm (Single peak fitting) and 6.6nm (Multiple peak fitting).

### 3.1.2 Determination of lattice parameters

For the cubic phase, the lattice parameters are related as:

$$\frac{1}{d^2} = \frac{h^2 + k^2 + l^2}{a^2}$$

And Unit Cell Volume is given by:

$$V = a^3$$

The calculated value of a is:

$$a = \sqrt{d^2(h^2 + k^2 + l^2)}$$

where d is the interplanar distance (Å)

a is the lattice parameter (Å)

(hkl) is the miller indices

Bragg's law is given by:

$$n\lambda = 2d\sin\theta$$

$$d = \frac{\lambda}{2 \sin \theta} = \frac{0.154}{2 \sin(\frac{35.27}{2})} = 2.54 \text{ \AA}$$

The lattice parameter was calculated with the data:

$$a = \sqrt{2.54298^2(3^2 + 1^2 + 1^2)}$$

$$= 8.4341 \text{ \AA}$$

For a cubic system, a=b=c

$$a=b=c=8.43 \text{ \AA}$$

Unit Cell Volume:

$$V = a^3$$

$$= 8.4341^3$$

$$= 599.9516 \text{ \AA}^3$$

The calculated values are in good accordance with the reported JCPDS data.

In comparison with the chemically synthesized sample, the current sample has got increased crystallinity. The average crystallite size of the current sample was observed to be less than 10 nm (Average: 7.135nm) which is very small compared to chemically derived ZnFe<sub>2</sub>O<sub>4</sub> nanoparticles synthesized under same conditions by sol-gel method, which aids for an increase in surface to volume ratio which is a catalyst for adsorption properties of ZnFe<sub>2</sub>O<sub>4</sub>.

It is also noted that both chemically and biologically synthesized  $\text{ZnFe}_2\text{O}_4$  samples have comparable unit cell characteristics.

### 3.2 IDENTIFICATION OF FUNCTIONAL GROUPS: FOURIER TRANSFORM INFRARED SPECTROSCOPY (FTIR)

The FTIR spectra analysis was acquired in a frequency range of  $400\text{-}4000\text{cm}^{-1}$ . Jasco Ft/IR-4600 model instrument was used for the analysis. The functional groups attached to the synthesized material were found by studying the absorption peaks.

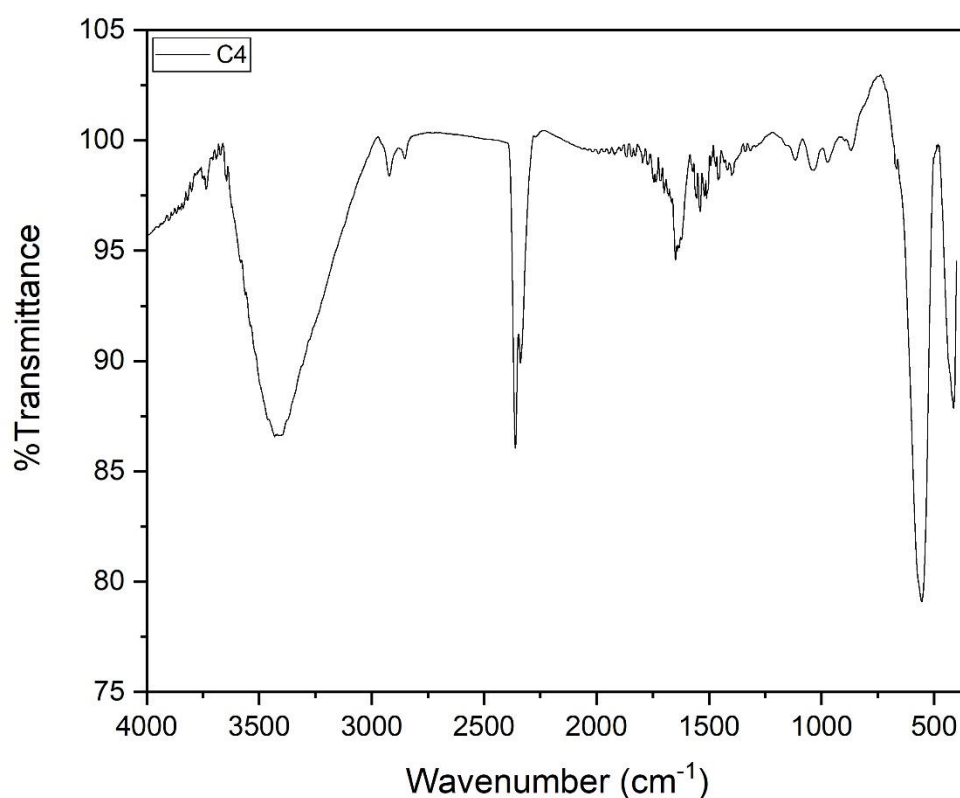


Fig 3.2: Fourier transform Infra-red pattern of  $\text{ZnFe}_2\text{O}_4$  nanoparticles

The broad peak in the range  $3420\text{ cm}^{-1}$  affirms the presence of (O-H) bond of surface hydroxyl groups of biomolecules, A weak peak around  $1643\text{ cm}^{-1}$  represents (C=O) stretching vibration and a peak in the range of  $1041\text{ cm}^{-1}$  represents (C-O-C) groups that resulted from the plant extracts<sup>[1][2]</sup>. The strong (Fe-O) absorption bands around  $569\text{ cm}^{-1}$  and



(Zn-O) band at  $415\text{ cm}^{-1}$  confirm that the main phase of synthesized particles is  $\text{ZnFe}_2\text{O}_4$  [3]. The peak located at  $2351\text{ cm}^{-1}$  indicates C=C stretching vibrations. The peak at  $693\text{ cm}^{-1}$  indicates Metal-Oxide (Fe-O) bonds [4].

Comparing the FTIR pattern with that of Sol-gel synthesized  $\text{ZnFe}_2\text{O}_4$  sample, presence of characteristic plant extract bonds is evident in biosynthesized sample which is absent in the former.

### 3.3 MORPHOLOGICAL STUDIES: SCANNING ELECTRON MICROSCOPE

The morphology of  $\text{ZnFe}_2\text{O}_4$  nanoparticles were recorded using GeminiSEM 300 model SEM instrument. A better morphology with less agglomeration is seen which can be due to the biomolecules present in the extract that act as the stabilizing agent [5]. The particle size was found to be  $22.97\text{ nm}$ .

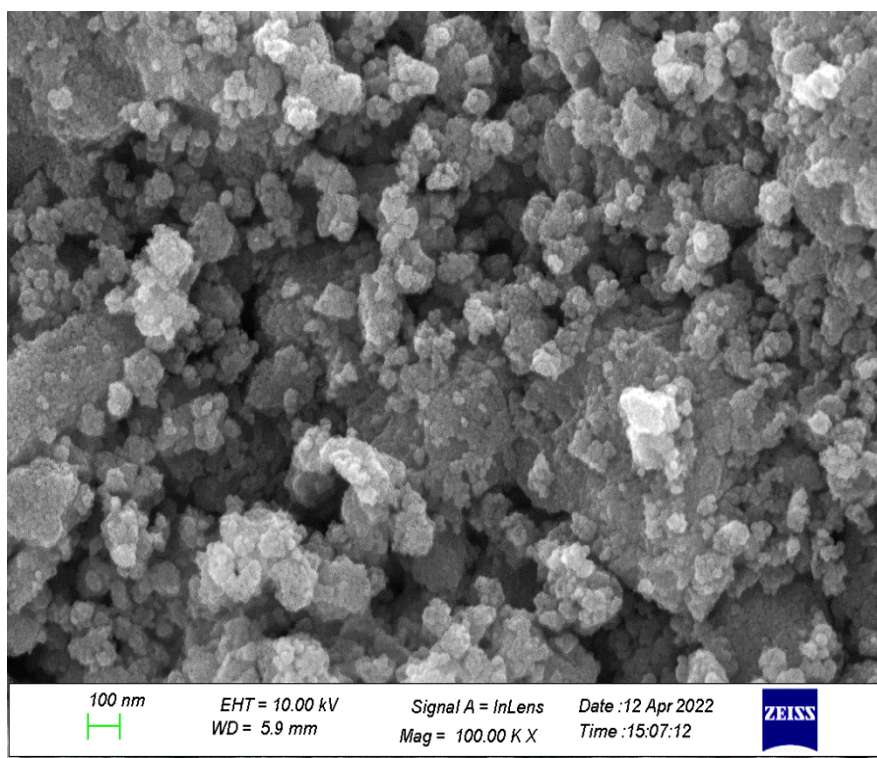


Fig 3.3 (a): SEM image of bio  $\text{ZnFe}_2\text{O}_4$  nanoparticles

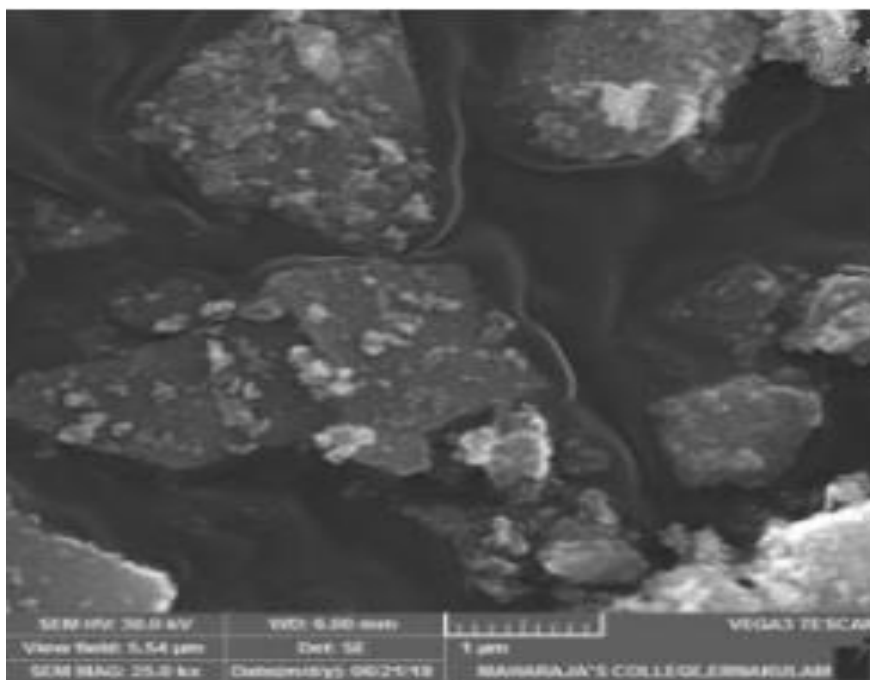


Fig 3.3 (b): SEM image of Sol-gel synthesized  $ZnFe_2O_4$ <sup>[6]</sup>.

Fig 3.3 (a) and Fig 3.3 (b) represent the morphology of biologically and chemically synthesized  $ZnFe_2O_4$  samples. In comparison, it is evident that the biologically synthesized  $ZnFe_2O_4$  particles are distributed uniformly with less agglomeration. The particles of bio  $ZnFe_2O_4$  possess a spherical morphology whereas  $ZnFe_2O_4$  (chemical) particles are of irregular shapes and sizes. The spherical nature of  $ZnFe_2O_4$  (bio) plays a major role in their adsorptive properties. Due to this, bio  $ZnFe_2O_4$  will possess more active sites for adsorption. Biosynthesis offers better particle size, stability, and mono dispersity<sup>[5]</sup>.

### 3.4 ADSORPTION STUDIES: ICP MS

Batch adsorption studies were carried out for the  $ZnFe_2O_4$  sample. The optimized values of <sup>[6]</sup> dosage of adsorbate and adsorbent were taken for the current study. The optimized value of the parameters such as temperature, adsorbent dosage, initial ion concentration, and contact time was taken and the adsorption efficiency and percentage removal calculated were compared with the result which is previously reported <sup>[6]</sup>. The whole experiment was done at room temperature (301 K), neutral pH for a contact time of 45 minutes.

20mL of 25 ppm Cr (VI) solution was taken as the working solution. After the contact time, the beaker was taken out and kept on top of a magnet for speedy settling. This was followed by filtration of the working solution whose Cr (VI) concentration was determined using ICP MS (model: Agilent 7800).

The percentage removal, the adsorption efficiency of Cr(VI) by Zinc ferrites were calculated using the equation:

$$\% = \frac{(C_i - C_{eq})}{C_i} \times 100$$

where  $C_i$  is the initial  $\text{Cr}^{6+}$  concentration and  $C_{eq}$  is the equilibrium concentration ( $\text{mgL}^{-1}$ ). This was compared with the reported data [6].

### **i) Contact time**

The working solution along with the  $\text{ZnFe}_2\text{O}_4$  adsorbents of 0.1 g was agitated for 45 minutes in a magnetic stirrer. After the contact time, the filtrate was collected and labeled as “CT-C”.

$$C_i = 25 \text{ ppm}$$

$$C_{eq} = 10.453 \text{ ppm}$$

$$\begin{aligned} \% &= \frac{(25 - 10.453)}{25} \times 100 \\ &= 58.18\% \end{aligned}$$

### **ii) Temperature**

0.25g of  $\text{ZnFe}_2\text{O}_4$  sample was put in the working solution and it was stirred for a contact time of 45 minutes. The filtrate obtained was labeled “TP-C”.

$$C_i = 25 \text{ ppm}$$

$$C_{eq} = 3.046 \text{ ppm}$$

$$\begin{aligned} \% &= \frac{(25 - 3.046)}{25} \times 100 \\ &= 87.81\% \end{aligned}$$

### **iii) Adsorbent dosage**

The adsorbent dosage to the working solution was 1 g which was agitated for 45 minutes. The filtrate collected was labeled as “AD-C”.

$$C_i = 25 \text{ ppm}$$

$$C_{eq} = 0.982 \text{ ppm}$$

$$\begin{aligned} \% &= \frac{(25 - 0.982)}{25} \times 100 \\ &= 96.07\% \end{aligned}$$

#### iv) Initial Ion Concentration

20 mL of 10 ppm solution was taken as the working solution onto which 0.25 g of ZnFe<sub>2</sub>O<sub>4</sub> adsorbents were added. This was agitated for 45 minutes. The filtrate obtained after the contact time was named “IIC-C”.

$$C_i = 25 \text{ ppm}$$

$$C_{eq} = 0.559 \text{ ppm}$$

$$\% = \frac{(25 - 0.559)}{25} \times 100$$
$$= 94.41\%$$

The ICP MS data of equilibrium concentration of Cr<sup>6+</sup> after the contact time is shown below:

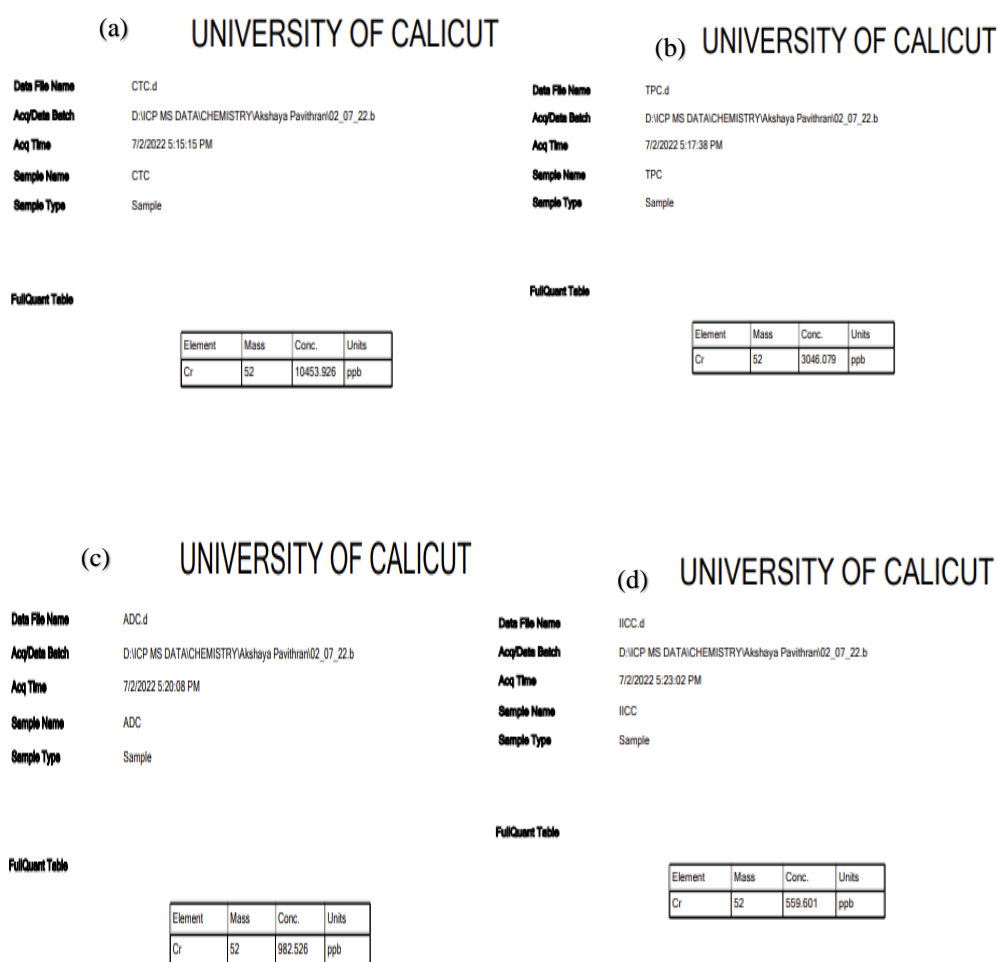


Fig 3.4 (a), (b), (c), (d): Equilibrium concentration of Cr<sup>6+</sup> for contact time, temperature, adsorbent dosage, and initial ion concentration respectively.

The adsorption efficiency of bio ZnFe<sub>2</sub>O<sub>4</sub> and sol-gel-derived ZnFe<sub>2</sub>O<sub>4</sub> is compared in the following table:

Parameters	Adsorbent dosage in g	Initial Cr <sup>6+</sup> concentration in ppm	Equilibrium Cr <sup>6+</sup> Concentration in ppm	Adsorption Efficiency (%)	
				Chemical Synthesis: Sol-gel method	BIO SYNTHESIS : Co-Precipitation Method
Contact Time	0.1	25	10.453	53.89	58.18
Temperature	0.25	25	3.046	65.95	87.81
Adsorbent Dosage	1	25	0.982	92.62	96.07
Initial Ion Concentration	0.25	10	0.559	87.8	94.41

Table 2: Comparison of adsorption efficiency

The adsorption efficiency of Cr(VI) of bio-synthesized ZnFe<sub>2</sub>O<sub>4</sub> nanoparticles is greater than what is shown by the chemically synthesized samples. Crystallite size and the concentration of surface hydroxyl groups have a great influence on the adsorption capacity of metal ferrites. This is because of increased electrostatic interaction and intra-sphere complexation on adsorption behavior<sup>[7]</sup>. Materials with a small particle size will have a developed surface as most of the atoms occupies on the surface contribute much to the adsorption process<sup>[7]</sup>. The presence of surface hydroxyl groups aids the adsorption process<sup>[8]</sup>.

The adsorptive behavior of a sample depends on various factors. They are crystallinity, morphology, crystallite size, and concentration of surface hydroxyl groups. In the present work, the sample possesses high crystallinity, a low average crystallite size of less than 10nm, spherical morphology, and surface hydroxyl groups. The desorption analysis of spent adsorbents is in progress.

## REFERENCES

- 1) Hafez Ghoran, Salar, et al. "Biosynthesis of zinc ferrite nanoparticles using polyphenol-rich extract of Citrus aurantium flowers." *Nanomedicine Research Journal* 5.1 (2020): 20-28.
- 2) Welegergs, G. G., et al. "Electrochemical properties of green synthesised Zinc oxide (ZnO) Nanoparticles." *MRS Advances* 5.21-22 (2020): 1103-1112.
- 3) Wan, Jiaqi, et al. "Facile synthesis of zinc ferrite nanoparticles as non-lanthanide T 1 MRI contrast agents." *Journal of Materials Chemistry* 22.27 (2012): 13500-13505.
- 4) Welegergs, G. G., et al. "Electrochemical properties of green synthesised Zinc oxide (ZnO) Nanoparticles." *MRS Advances* 5.21-22 (2020): 1103-1112.
- 5) Muthukumar, Harshiny, et al. "Plant extract mediated synthesis enhanced the functional properties of silver ferrite nanoparticles over chemical mediated synthesis." *Biotechnology Reports* 26 (2020): e00469.
- 6) Nizam, Thanooja, et al. "Adsorption efficiency of sol-gel derived nano metal ferrites, MFe<sub>2</sub>O<sub>4</sub> (M= Ni, Zn, Cu) on the removal of Cr (VI) ions from aqueous solution." *Journal of Sol-Gel Science and Technology* 101.3 (2022): 618-629.
- 7) Ivanets, Andrei, et al. "A comparative study on the synthesis of magnesium ferrite for the adsorption of metal ions: Insights into the essential role of crystallite size and surface hydroxyl groups." *Chemical Engineering Journal* 411 (2021): 128523.
- 8) Kaur, Amrit, et al. "Sustainable preparation of Fe (OH) <sub>3</sub> and α-Fe<sub>2</sub>O<sub>3</sub> nanoparticles employing Acacia catechu extract for efficient removal of chromium (VI) from aqueous solution." *Environmental Nanotechnology, Monitoring & Management* 16 (2021): 100593.

## CONCLUSION

Water scarcity has become a major issue and several methods are being employed for the treatment of wastewater. One such effective method is by employing adsorption by metal ferrites. It's previously reported that  $\text{ZnFe}_2\text{O}_4$  nanoparticles show high adsorptive efficiency. The present work focuses on the biosynthesis of  $\text{ZnFe}_2\text{O}_4$  nanoparticles and their adsorptive properties towards Cr(VI) ions which is a major heavy metal that causes water contamination.

$\text{ZnFe}_2\text{O}_4$  nanoparticles were successfully synthesized by the plant extract mediated co-precipitation method. The calcination temperature was optimized by analyzing the XRD patterns of the synthesized  $\text{ZnFe}_2\text{O}_4$  nanoparticles calcined at different temperatures. The crystallite size was calculated and was found to be less than 10nm which is much less than that of the chemically synthesized  $\text{ZnFe}_2\text{O}_4$  sample. SEM image confirmed that the ferrite nanoparticles are less agglomerated and have spherical symmetry.

The adsorptive properties of biosynthesized  $\text{ZnFe}_2\text{O}_4$  nanoparticles were studied and compared with sol-gel-derived  $\text{ZnFe}_2\text{O}_4$  nanoparticles. The optimized values of the factors that affect the adsorption process (Contact time, temperature, adsorbent dosage, and initial ion concentration) were taken and respective adsorption efficiency was calculated from the final concentration of Cr(VI) obtained from ICP MS after the adsorption process. The biosynthesized samples show higher adsorption efficiency than the chemically synthesized ferrite samples. This can be attributed to lower crystallite size, better morphology, and the concentration of surface hydroxyl groups due to the active groups present in the plant extracts.

## FUTURE SCOPE

Bio synthesized ferrites have hence proved their efficiency in heavy metal removal. The present work is a comparative study with chemically synthesized  $\text{ZnFe}_2\text{O}_4$  whose adsorptive properties are previously reported. As bio synthesized samples show high adsorption efficiency of Cr(VI) ions, the factors affecting the adsorption process (pH, contact time, temperature, adsorbent dosage, and the initial ion concentration) is to be optimized, where the maximum intake of the metal ions will take place. In the current work, the optimized values reported previously have been taken to study the adsorptive properties of the biosynthesized ferrite sample.

The high intake of the metal ions onto the ferrite surface has drawn attention to the porous nature and the surface area of the biosynthesized ferrites. This can be understood by employing Brunauer, Emmett, and Teller (BET) technique. The morphology of the  $\text{ZnFe}_2\text{O}_4$  sample has enhanced the adsorptive properties, so more studies based on its spherical morphology have to be made and all possibilities it offers.

Further studies is to be made to study the properties of plant-mediated synthesized ferrite samples, thus by making them the most efficient adsorbents which include:

1. Optimization of all parameters affecting the adsorptive property of  $\text{ZnFe}_2\text{O}_4$
2. Desorption studies
3. Magnetic studies by employing Vibrating sample magnetometer (VSM)
4. BET analysis which gives the porous nature of the ferrites.